UNIVERSITY OF NAPLES "FEDERICO II"

DOCTORATE
MOLECULAR MEDICINE AND MEDICAL BIOTECHNOLOGY
XXIX CYCLE

TITLE

Distribution and evolution of methylation profiles in mouse brain cells.

TUTOR
Prof. Lorenzo Chiariotti

CANDIDATE
Dr. Ermanno Florio

COORDINATOR
Prof. Vittorio Enrico Avvedimento

ACADEMIC YEAR
2015-2016

INDEX

ABSTRACT

The methylation profiles generated during the early stages of mouse brain development play a critical role in the gene expression regulation program; given the large number of different cellular population in murine brain, is the great importance the study of the cell to cell heterogeneity in terms of DNA methylation. In this work, I performed an in-depth single molecule methylation analysis in order to assess the cell to cell methylation heterogeneity analyzing the epialleles composition at the D-aspartate oxidase (*ddo*) putative regulatory region, that is a gene implicated in a correct neurodevelopment and that undergoes a strong methylation changes during the early stages of mouse development. I found that brain methylation heterogeneity is generated and develops in an extremely conserved fashion, giving rise to a deterministically regulated distribution of different epialleles, distinct for each stage and cell type, evoking the possible existence of a novel, cell population based, combinatorial code of CpG methylation. Importantly, rapid epialleles remodeling toward mature neuronal and glial patterns was observed in ES cells population upon neural differentiation. The high degree of epipolimorphism, detected also in pure cell populations, supports the existence of mechanisms oriented to maintain the epiallele patterns in a dynamic equilibrium involving continuously occurring methylation and demethylation events in each single cell. The interplay between contiguous CpGs differing in methylation susceptibility likely underlies specific epiallele frequency and dynamics in a spatial-specific manner. The present data on *Ddo* gene provide a proof of principle that employment of high coverage single molecule methylation analysis, may potentially reveal unprecedented mechanisms underlying methylation establishment, changes and alterations within cell populations in development and diseases, unpredictable by classical methylation analyses.

ABBREVIATIONS

Ddo:	D-aspartate oxidase
CpG:	C--phosphate--G
ncRNA:	Non coding RNA
siRNA:	Small interfering RNA
piRNA:	RNA Piwi-interacting
miRNA:	microRNA
lncRNA:	Long non coding RNA
DNA:	Deoxyribonucliec Acid
DNMT:	DNA methyltransferase
RNA:	Ribonucleic acid
TET:	Ten-eleven translocation
PCR:	Polymerase Chain Reaction
MSP:	Methyl Specific PCR
NGS:	Next generation sequencing
Ct:	Threshold cycle
WGBS:	Whole genome bisulfite sequencing
RRBS:	Reduced representation bisulfite sequencing
BDNF IV:	Brain-derived neurotrophic factor
CDKL5:	Cyclin-dependent kinase-like 5
MeCP2 :	Methyl CpG binding protein 2
Dlx5:	Distal-less homeobox 5
FXYD1:	FXYD domain containing ion transport regulator 1
FOX G1:	Forkhead box protein G1
HIPP:	Hippocampus
CX:	Cortex
PFC:	Prefrontal cortex
CB:	Cerebellum
ST:	Striatum

INTRODUCTION

1.1 Epigenetic mechanism.

The story of Biology teaches us that during the development of mammals, nothing is left to the case, especially the gene expression. Among the main players of gene regulation, surely there are the epigenetic mechanisms (1). Epigenetics is the branch of the science that studies the heritable modifications not involving DNA nucleotide sequence (2) (Fig.1); three different kind of regulation subtend epigenetic changes: chromatin modifications (3, 4), noncoding RNA (5, 6), and DNA methylation (7). For what concern the chromatin epigenetics, the most common modifications are those borne by histone lysines (acetylation and methylation) (8). These modifications are the most important system to regulate the tissue-specific gene expression patterns and global gene silencing (9). After the fertilization, one of the main roles of histone methylation is to keep the differences or the asymmetry between paternal and maternal genomes. The maternal genome is more abundant in Lysine methylation, as H3K9me2-3, H3K27, H3K4me3 (10, 11) than the paternal. The paternal one is characterized by the H4 hyperacetylation and H3K9me1 (12, 13). Instead, the second class of epigenetics area encloses the non-coding RNA (ncRNA); they are functional RNA molecules that are transcribed from DNA but not translated into proteins. They include siRNA, piRNA, miRNA, and lncRNA. It's well known that the short and long noncoding RNA are implicated in heterochromatin formation, DNA methylation targeting, gene silencing and histone modification (14-20). Last but not least, the DNA methylation is one of the most complicated mechanisms that subtends the regulation of gene expression especially during the brain development of mammals (21, 22). The critical role of DNA methylation in neurodevelopment of mammals brain is highlighted by the absence of methyl-CpG binding protein 2 (MECP2), a reader of DNA methylation status. Indeed, its absence or mutation during the early stage of development may generate a strong cognitive deficit in the human brain (23, 24). So, as the methyl CpG readers are very important in human development, the enzymes involved in DNA methylation generation and maintenance are definitely among the

principal actors that play a crucial role in brain development. Moreover, the DNA methylation processes are implicated in many brain function as learning (25), memory formation and maintenance (26) and neuronal plasticity (27). Furthermore, It has been demonstrated that the alterations of DNA methylation patterns are also implicated in neurodegenerative and neuropsychiatric disease (28-32), highlighting the importance of correct formation and preservation of DNA methylation patterns in brain cells.

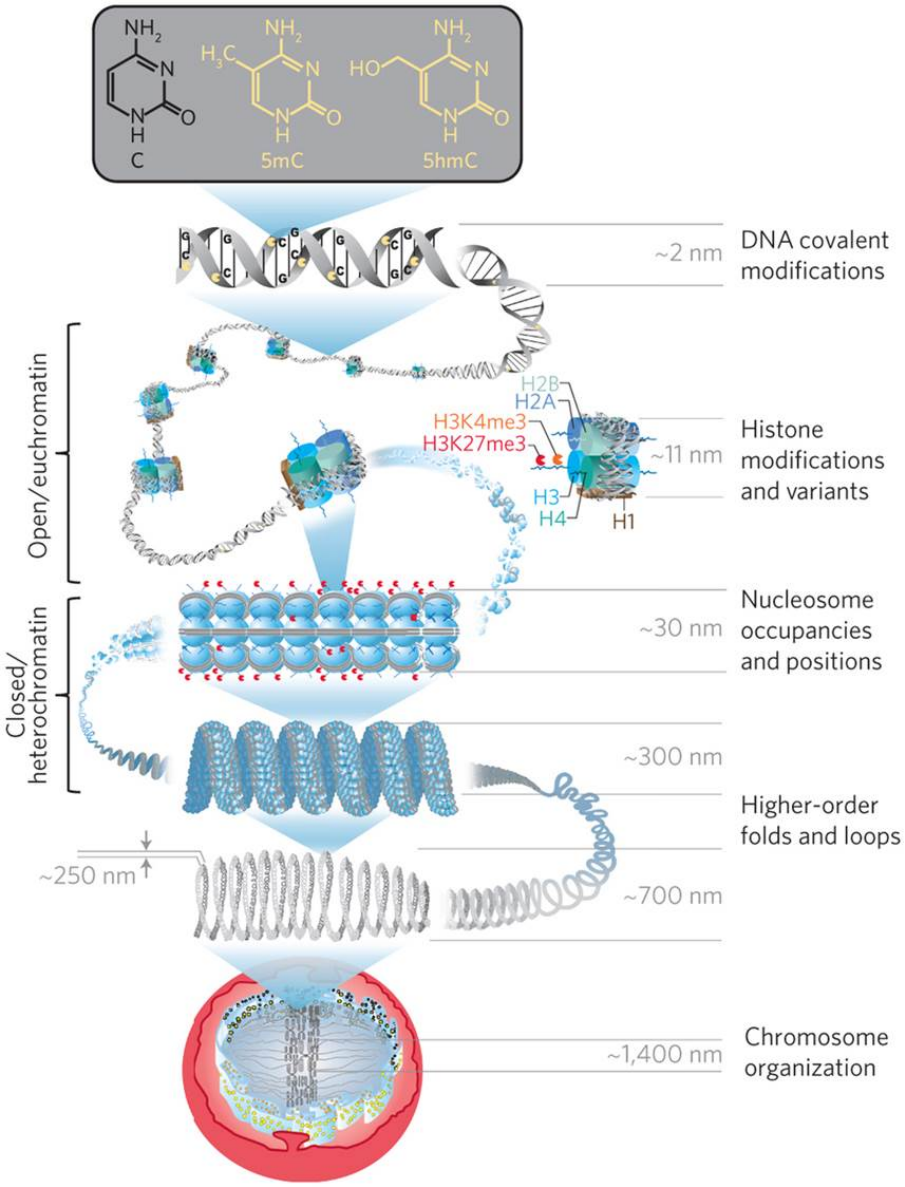

Figure 1. The root layer is the DNA sequence containing covalent modifications such as cytosine methylation (5mC) and hydroxymethylcytosine (5hmC). The black structure is an unmodified cytosine base. The DNA is then wrapped around octameric histone proteins into nucleosomes and into chromatin. The nucleosomal histones H2A, H2B, H3 and H4 form pairs with one H3–H4 tetramer and two H2A–H2B dimers and can be exchanged with variants or chemically modified on their protruding tails such as histone 3–lysine 27 trimethylation (H3K27me3). The structure of the chromatin is mediated by the nucleosome packing with open/euchromatin having fewer nucleosomes positioned than closed/heterochromatin. The condensed heterochromatin has been shown to possess a unique solenoid structure and higher-order loops and folds also exist to further compact the chromatin into chromosomes. The various layers and modifications establish whether the gene and the regulatory components (promoter, enhancer) are accessible and transcribed or inactive. (From Aguilar et al. Nature Ref: 93)

1.2 The DNA methylation

The cell-specific gene expression is a process that is finely regulated by epigenetic mechanisms. The ways in which this may happen are still unclear, but it's known that the DNA methylation plays a key role in these processes. For this reason, during the last years, the modalities of generation and maintenance of DNA methylation have been the most central topic in the epigenetic field. As know, the functions of DNA methylation include the gene regulation, genomic stability and chromatin structure (33). Its role in prokaryotic systems is to defend the host DNA from restriction enzyme digestion (34), while in mammalian cells and not only, the functions of DNA methylation include, in addition to the gene regulation, X inactivation(35-36), genomic imprinting (37), DNA mismatch repair (38) and DNA replication (39). Most of these processes are due to methylation of cytosine base present in the CpG dinucleotide, and the enzymes that perform this activity are defined as the family of DNMT protein. There are two classes of DNMTs: *de novo* and maintenance DNMTs. The de novo DNA methyltransferases DNMT3A and DNMT3B are implicated in cytosine methylation of unmethylated CpG sites (40), while DNMT1 is related to the maintenance of the DNA methylation pattern during DNA replication (41). Using a restriction endonuclease accessibility assays in isolated cell nuclei it was possible to demonstrate the presence of the DNA methylation (42). The evidence obtained from this experiment suggested the existence of specific proteins that may able to binding the methylated CpGs. Indeed, after few years, the family of Methyl Binding Protein was discovered. The most studied protein of this family is MeCP2, a protein capable of recognizing single methyl-CpG dinucleotides (43), considered one most important protein implicated in a correct mammals brain development. Indeed, altered sequence or amount of MeCP2 protein in the brain (due to sequence mutations), is related to severe neurological disorders (44). Others relevant methylation modification on cytosine no paired with a guanosine CT, CC, CA, were also found; they are called non-CpG methylation (45). The non CpG methylation could play a crucial role in brain development, indeed, their levels are high in embryonic stem (ES) but are largely lost

upon cell differentiation (46, 47). Moreover, the mCH levels are nearly absent in fetal cortex, vice versa they are copious in the adult frontal cortex (48). The mCH functions could be related to expression regulation as suggested by findings that in mammalian brain these modifications are depleted in expressed genes, with genic mCH level inversely proportional to the abundance of the associated transcripts (49). Moreover, the cytosine, in the context of CpG dinucleotides, can be found in a different modification status, that include the carboxi-, formyl- and hydroximethylated ones. These intermediate forms are produced by TET enzymes family (50, 51). These cytosine modifications could be part of an active DNA demethylation pathway (52). In brain, hydroximethylcytosine seems to be more abundant in neurons, rather than glial cells, and, although its role is still unclear, it was shown to be essential to obtain a correct brain development (48). Thus, the continuous flow of methylation and demethylation processes is likely essential for the correct development of mammals brain and only at the end of this modelling process, each type of brain cells will acquire a cell type-specific methylation profile becoming able to regulate the exact gene expression program. Indeed, the differences of epigenetic features between glia and neuron cells could be one of the principles that characterize the neural diversity (53).

1.3 How to study the DNA methylation in NEXT GENERATION SEQUENCING age

Methods to investigate DNA methylation are multiple, it is possible to divide into three main categories: i) techniques based on bisulphite conversion (54), ii) based on digestion performed by restriction enzymes that are sensible to the methylation CpG status of and iii) based on the immunoprecipitation of the methyl group. The gold standard method to investigate the DNA methylation status is the bisulfite DNA conversion followed by different kind of analyses. Using this method the unmethylated cytosine (C) is converted into uracil residues (U) while methylated cytosines remain unmodified (54). After this treatment, the detection of DNA methylation can be achieved by PCR (55), sanger sequencing (56), microarray (57) or next generation sequencing (58). The MSP (methylation specific PCR) is based on the use of two

couple of primers, one able to identify the unmethylated CpGs and the other one amplifies the methylated DNA (59). The methylation status of the analyzed region can be evaluated comparing the Ct derived from two Real time PCR reactions (one for each couple of primers, methylated or unmethylated). The classical Sanger sequencing involves the analysis of cloned PCR products: the bisulfite DNA is first amplified by specific primers, amplified fragments are cloned and then about 20-30 clones are subject to sequence analysis (60). The evolution of sequencing techniques, which improved the resolution of bisulfite analysis, was the pyrosequencing which is used to obtain a more quantitative DNA methylation information, and allows to detect even small differences in methylation average (61). Chip-arrays, specific for bisulfite treated genomic DNA, may include a large number of selected CpGs (typically half a million), and may produce an overview of genome-wide methylation status (62). Recently, the advent of the sequencer of latest generation has redefined the study of DNA methylation. The whole genome bisulfite sequencing (WGBS) produces an enormous amount of methylation data than ever before (63). The use of sequencer as Roche 454 or Illumina Hiseq, allows to analyze the methylation status of the entire genome, making the bisulfite process followed by NGS the best technique to study the DNA methylation in different fields as tumor progression (64), neurodegenerative diseases (65), development (66) and many more. All these methods to evaluate the DNA methylation are able to obtain an accurate average methylation, some of these even all along the genome. However, the main limitation is the low coverage that do not allow to detect and measure cell to cell heterogeneity within a given cell population. among the different cell populations. In the next paragraph I will describe a novel approach, which includes an ultra-deep methylation analysis followed by an ad hoc generated bioinformatics-analysis, that was developed in my lab to overcome these limitations and was applied to the study of epiallele generation and evolution in brain cells during development and neural differentiation.

1.4 Cell to Cell heterogeneity and the epialleles analysis.

Epigenetic profiles are sculpted during development and, in particular, DNA methylation landscape of mammalian brain cells is dynamically reconfigured through development (27, 48, 67). Such reconfiguration occurs, at brain specific genes, prevalently during the late stages of embryogenesis and early post-natal developmental period leading to critical changes in the gene expression program that, once the process come to end, is thought to be maintained throughout the life. A progressive shaping of DNA methylation patterns occurs in a regulated manner, both at CpG and CpH sites, mainly in a specific time-window around the birth possibly providing an epigenetic memory specific for each type of brain cells (48). Such phenomenon, crucial to complete embryonic development, is the result of a dynamic interplay between DNA methylation and demethylation events assisted by different DNA methyltransferases or by Ten-eleven translocation enzymes. At genomic level, as a result of these processes, each type of brain cells, despite sharing similar global mCpG content, acquire a cell-type specific genomic DNA methylation landscape that gives an identity card for different brain cells and govern and stabilize an elected gene expression program. Indeed, in a recent comprehensive study using a novel cell separation approach, Mo et al. (53) found that glial cells and three different subtypes of neocortical neurons show very distinctive epigenomic signatures including CpG and CpH methylation state at promoters and intragenic regions which associate with gene specific activity, and concluded that epigenomic landscape reflect neuronal diversity. Appropriate patterns of DNA methylation in the brain play an important role in mental health (29, 68). Several pivotal gene-specific or genome-wide studies addressing alteration of DNA methylation in animal models or post-mortem brain of psychiatric subjects, nicely revealed the association of altered average CpG methylation at certain genes with specific psychiatric condition (28, 30, 69-71) or negative stressors (32, 72) confirming the importance of correct formation and preservation of DNA methylation patterns for brain functions and the role of altered configuration of brain DNA methylation profiles in the pathogenesis of psychiatric disorders. The vast majority of these studies, regardless of the techniques employed, took into consideration the average amount of

CpGs methylation in specific genomic regions or their genome-wide distribution with a only relatively high resolution. However, mammalian genome contains about 29 million of CpG sites which are non-randomly distributed along the genome. Because each of CpG sites may exist in a methylated or unmethylated state, the number of possible combinations is huge ($10^{8,700,000}$) and may therefore enormously increase the potential information content of genomic DNA, without considering here the further increase provided by other cytosine modifications such as hydroxymethylation and non CpG methylation. Although at genomic level it is practically impossible, or at least a very hard task, to verify all the possible mCpG combinations present in brain cells, in principle each cell may bear a specific combination of methylated CpG at specific loci that may reflect the origin of the cell and/or the functional state of a given gene (allele) in that cell. This introduce the concept of "epipolymorphism" which goes far beyond the simple identification of differentially methylated regions, by means that brain cells may be considered a population of epigenetically heterogeneous cells in which each combination of mCpG at a given locus represents a specific epiallele. Such information is lost when the average methylation, even at single CpG sites, is evaluated. Nevertheless, although only a low number of molecules/locus (about ten to fifty) is usually analyzed both in gene-specific and genome-wide studies, most of previous studies based on bisulfite sequencing revealed that different combinations of mCpG are indeed present at given loci. These are usually interpreted as the effect of stochastic methylation and demethylation events resulting in an average methylation degree which is then associated to gene activity. However, it should be taken into consideration that each of the detected profile corresponds to the configuration of a single allele, in single cells belonging to the cell mixture present in an analyzed tissue. By genome-wide approaches, recent works, based on comparing the methylation of few adjacent CpGs, have addressed the heterogeneous methylation accounting for cell to cell methylation variability in liver (73), in leukemias (74) and in immortalized fibroblasts (75) nicely describe the stochastic and clonal evolution of epialleles during carcinogenesis.

AIM OF THESIS.

2.1

It is known that the balance between DNA methylation and demethylation events are important phenomena that influence the correct development of the mammalian brain. It is also known that the epigenetic mechanisms are heavily implicated in the generation and progression of neuropsychiatric and neurodegenerative disorders. However, little it is known about the cell-to cell heterogeneity of methylation profiles and how much this phenomenon occur in a stochastic or a well-orchestrated fashion. During my Ph.D. course, I investigated, by very high coverage methylation analyses, if a cell to cell methylation variability exists in brain and whether this variability represents the result of stochastic events or a genetically and/or environmentally driven phenomenon, developmentally regulated, leading to an orchestrated distribution of epialleles among the entire population of brain cells. In order to gain a proof-of-principle that precise analysis of variable frequencies of multiple patterns (epialleles) may help to answer these questions, I chose to perform an ultra-deep methylation analysis (coverage 200.000-300.000 reads/sample) of a single locus. I found that brain epi-polymorphisms are generated and develop in an extremely conserved fashion giving rise to a deterministically regulated distribution of different epialleles, evoking the possible existence of a novel combinatorial code of CpG methylation within cell populations. The finding of highly conserved epigenetic diversity, retained in purified cell populations, supports the possible existence of mechanisms oriented to maintain the epigenetic system in a dynamic stability. My results encourage the employment of this novel approach to study DNA methylation since it may potentially give important information on cell identity and origin, functional state of a given gene and on the mechanisms underlying DNA methylation establishment, changes and, potentially, alterations of these processes in diseases.

MATERIAL AND METHODS

3.1 Collection of mouse brain tissue.

In my study, all brain tissues were collected from C57BL/6J (bought from Jackson Laboratory; Bar Harbour, ME).The mice were grown in the CE.IN.GE's laboratories as in Punzo et.al (76). All research involving animals was performed in accordance with the European directive 86/609/EEC governing animal welfare and protection, which is acknowledged by the Italian Legislative Decree no. 116 (January 27, 1992). Animal research protocols were also reviewed and consented by a local animal care committee. I used half brain from each of 3 mice from different developmental stages: Embryonal day 15 (E15), Post Natal day 1 (P0), P15, P30, and P60. To study the methylation profile among the different brain areas, I collected 5 brain areas from two mice at P30 Stage (prefrontal cortex, cortex, hippocampus, cerebellum, and striatum). All tissue samples were pulverized in liquid nitrogen and stored at -80°C before use.

3.2 Cell isolation and its treatments.

Primary Cortical Neurons. Cortical neurons were prepared from brains of 17-day-old C57BL/6J mouse embryos, as previously described (77). Briefly, mice were first anesthetized and then killed by cervical dislocation to minimize the animals‘ pain and distress. Dissection and dissociation were performed in Ca2/Mg2-free buffer saline (HBSS). Tissues were incubated with trypsin for 20 min at 37°C and dissociated by trituration in culture medium. Cells were plated at 3.5-5 x 106 in 60 mm plastic Petri dishes, precoated with poly-D-lysine (20 mg/ml), in MEM/F12 (Invitrogen, Carlsbad, CA) containing glucose, 5% deactivated FBS, and 5% horse serum (Invitrogen), glutamine, and antibiotics. Ara-C (10 mM) was added within 48 h of plating to prevent non-neuronal cell growth. Neurons were cultured at 37°C in a humidified 5% CO2 atmosphere. All the experiments on primary cortical neurons were performed according to the procedures described in experimental protocols approved by the Ethical Committee of the Federico II University of Naples.

Primary microglia, oligodendrocytes, and astrocytes isolation from mixed glial cell cultures.

Purified microglia, oligodendrocyte, and astrocyte cells were prepared from primary mouse mixed glial cells as previously described (78, 79). Briefly, cerebral cortices isolated from post-natal day 1 mouse brain were first dissociated enzymatically in a solution containing 0.125% trypsin and 1.5 mg/mL DNase (Sigma-Aldrich, St. Louis, MO) and then mechanically in Dulbecco‘s modified Eagle‘s medium supplemented with 10% fetal bovine serum, 1% penicillin-streptomycin, 2 mmol/L L-glutamine (Invitrogen). The cell pellet was resuspended and plated in tissue culture flasks in a normal medium at 37°C in a humidified, 5% CO2 incubator. After 12-15 days, the microglia cells were separated by a mechanical shaking of flasks on an orbital shaker for 60 min at 200 rpm at 37°C. The suspension containing microglia was centrifuged at 1000 rpm for 5 min and the pellet stored at -80°C. This procedure yielded 98% IB4-FITC or OX42-positive cells. To isolate oligodendrocyte lineage cells, the cultures were then subjected to an additional 16 h of shaking at 200 rpm. To minimize contamination by microglial cells, the suspension of detached cells was incubated twice for 40 minutes at room temperature. The non-adhering oligodendrocytes were centrifuged at 1000 rpm for 5 min and the pellet stored at -80°C. This procedure yielded 98% NG2-positive cells. Finally, the remaining confluent astrocytes were washed, scraped, centrifuged, and the pellets stored at -80°C until further analysis. This procedure yielded 98% GFAP -positive cells.

Embryonic stem cells. In vitro differentiation toward neurons and glia cells was performed as previously described (80). Briefly, at day 0, wild type TBV (129/SvP) ESCs were dissociated into a single-cell suspension and 1000 cells/cm2 were plated on gelatin-coated plates. The culture medium was replaced daily during the differentiation process.

Immortalized cells. A1 mes c-myc (A1) is a cell line immortalized by means of infection with a c-myc carrying retroviral vector of a primary mouse mesencephalon derived cells culture prepared from 11-day-old embryos (E11) as previously described (81). These cells proliferate and remain undifferentiated when grown in MEM/F12 (Invitrogen, Milan, Italy) supplemented with 10% FBS (HyClone, Milan, Italy).

3.3 DNA and RNA extraction protocols.

DNA was extracted from a portion of liquid nitrogen–pulverized tissue or cell pellets. DNA was prepared using DNeasy® Blood & Tissue Kit (Qiagen, Hilden, Germany), following the manufacturer‘s instructions. Total mRNAs were extracted using TRI REAGENT® (Invitrogen) solution, according to the manufacturer′s instructions. DNA and RNA were quality checked by 260/280 absorbance ratio using NanoDrop 2000, (Thermo Scientific) and were quantified using respectively Qubit® 2.0 Fluorometer with the dsDNA broad range assay kit (Invitrogen, Q32850) and Nanodrop 2000 (RNA).

3.4 cDNA and Real Time experiments.

One microgram of total mRNA of each sample was reverse transcribed with the QuantiTect Reverse Transcription kit (Qiagen) using an optimized blend of oligo-dT and random primers, according to the manufacturer’s instructions. All Relative Quantitative PCR were performed using ROCHE 480 instrument in 96-well plates. To calculate the relative expression levels I used the 2 -^{DD}CT method and all genes were normalized with GAPDH expression levels.

3.5 Bisulfite treatment

Bisulfite treatment was performed using EZ DNA Methylation Kit (Zymo Research). Genomic DNA (2 µg) was converted with ―C/T conversion reagent‖ and eluted in 50 µl of H2O following the manufacturer‘s instruction. To estimate the rate of bisulfite conversion, I used a spike-in control prepared by adding fully unmethylated M13mp18 double strand DNA (New England BioLabs) in 10 representative samples. After the library sequencing, I evaluated the conversion bisulfite of my experiments around 98-99%,

3.6 Amplicon Library preparation

To study the DNA methylation average and the epialleles distribution among different samples, I developed a double steps PCR strategy to generate a high quality of bisulfite amplicon library (Fig. 2). After the bisulfite treatment the DNA undergoes the first step of PCR reaction, I used a couple of tiled primers to generate products ranging in size from 300-450 bp. Table 1 shows all primers sequences used in this project. These primers contain an overhang adapter sequences at each 5'end (FW: 5' TCGTCGGCAGCGTCAGATGTGTATAAGAGACAG _3; RV: 5' GTCTCGTGGGCTCGGAGATGTGTATAAGAGACAG _3) that must be recognized in the second step of PCR. The first PCR conditions are: one cycle at 95°C for 2 min followed by 32 cycles at 95°C for 30 s, [primer Tm] for 40 s, 72°C for 50 s, followed by a final extension step at 72°C for 6 min. Reactions were performed in 30 µl total volumes: 3 µl 10x reaction buffer, 0.6 µl of 10 mM dNTP mix, 0.9 µl of 5 µM forward and reverse primers, 3.6 µl MgCl2 25 mM, 2-4 µl bisulfite template DNA, 0.25 µl FastStart Taq, and H2O up to a final volume of 30 µl. For both PCR steps, I used the FastStart High Fidelity PCR System (Roche). During this first part, there is a risk to produce a primers dimer, because each primer is long around 60 base. To avoid this formation, I performed an AMPure purification leveraging the magnetic Beads (Beckman-Coulter, Brea, CA). These magnetic beads are positively charged and are therefore capable of binding DNA if you use the right concentration. I prefer to use a ratio AMPure Beads/PCR products volume of 0.8 in order to delete as much as possible the dimers. After this first purification step, I checked each product size on 1.5% agarose gel. Then, I make the second step of PCR, to add multiplexing indices and Illumina sequencing adapters. The condition of second PCR step were as follows: 50 µl total volume, 5 µl 10x reaction buffer, 1 µl dNTP mix, 5 µl forward and reverse Nextera XT primers (Illumina, San Diego, CA), 6 µl 25 mM MgCl2, 5 µl of first PCR product, 0.4 µl FastStart Taq, and H2O up to a final volume of 50 µl. Thermocycler settings were: one cycle at 95°C for 2 min followed by 8 cycles at 95°C 30 s, 55°C for 40 s, 72°C for 40 s, followed by a final extension step at 72°C for 5 min. As before, I repeated one AMPure Beads purification this time with a different ratio 1.2 Beads/PCR.

The quantification process and the check of amplicon quality were performed respectively using Qubit® 2.0 Fluorometer and Agilent 2100 Bioanalyzer DNA 1000 Kit (Agilent Technologies, Santa Clara, CA), according to the manufacturer‘s instructions. The last step, it was the pooling of all PCR amplicons at an equimolar ratio. The amplicon library undergoes dilution to a final concentration of 8 picomolar. I decided to use a Phix control libraries (Illumina) [15% (v/v)] to increase the diversity of base calling during sequencing. According to the Illumina protocols, I sequenced all different amplicon library with a V3 reagents kits on Illumina MiSeq system (Illumina, San Diego, CA). Paired-end sequencing was carried out in 281 cycles per read (281 x 2). An average of 210,000 reads/sample were used for further analysis.

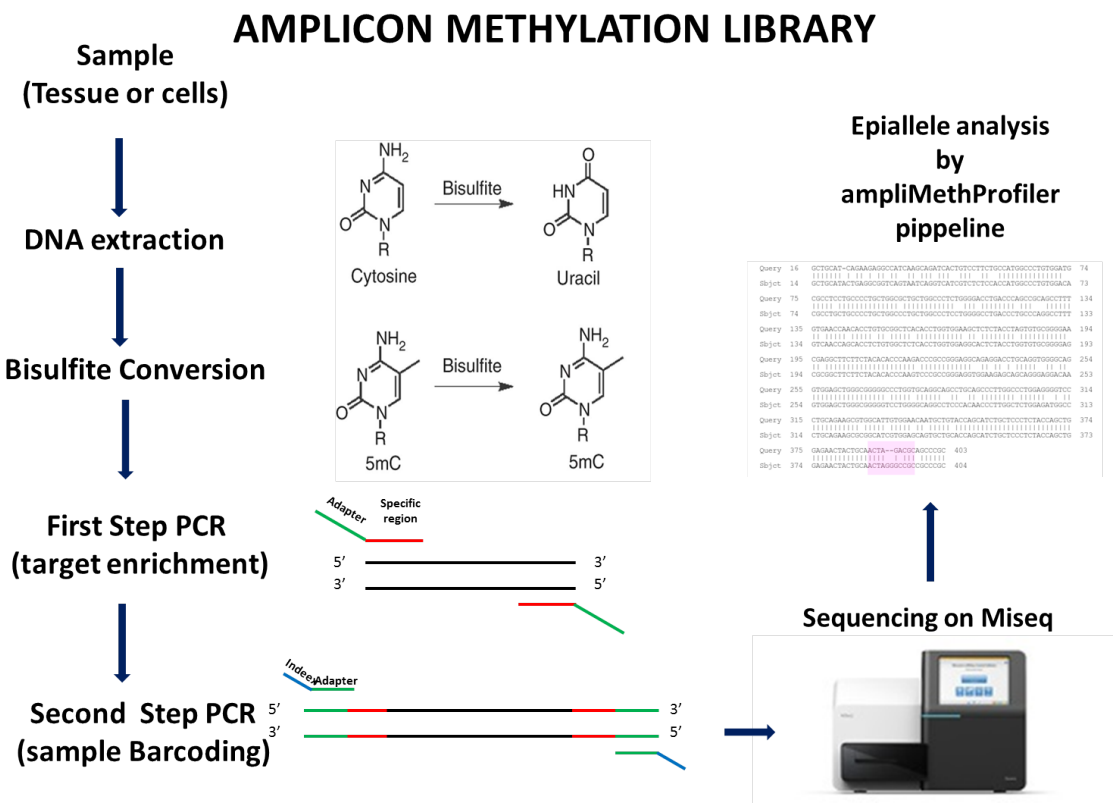

Figure 2. The scheme of strategy preparation of a amplicon methylation library.

Table 1.

GENE	AMPLICON	FW PRIMER	RV PRIMER
***Ddo* R1**	-2170/-1960	tttggtttttattTtTaaatTTtgata	AactAActatacatctcacttccctA
***Ddo* R2**	-1578/-1184	ggttagtggtttTtttgTagTTtttat	AAcattAtcccttcaAtccacaat
***Ddo* R3**	-927/-499	gTttttTTaTatgtTttggagTTt	acctccctAaaaAtcatttAattcta
***Ddo* R4**	-468/-63	gtgtgtttTtgaggaggtgaTaTtTa	aActtaccctccattAAtccatAcc
***Ddo* R5**	-229/+144	ggTtggtggTaagTtgaagttTttg	acccctaaaatcccaAaAtAcatac
***Ddo* R6**	+267/+671	TTtagtgttaaTttattagagTtgtgg	AAtacaatcccttcttAcaacaAAca
***Ddo* R7**	+801/+1201	gagggagttgggTatggagTaTaTata	AactctaAAAaAcaAacacaAaAAtc
M13 mp18	5946 / 6294	ggtgaagggtaattagttgttgtt	ccaataccaaacttacatacct

The capital letters in the primers sequences indicate the original C or G, respectively

3.7 Sequences handling

The Illumina Miseq sequencer platform produces two FASTQ files for each sample, one file contains the sequences from forward primer and one file with sequences from reverse primers. The first step to analyze the obtained sequences was evaluate the quality of each "read" using the FASTQC programme. Then in order to acquire one unique FASTQ file, I used a PEAR tool (82) by selecting a minimum range of overlapping residues of 40 and like a quality threshold a mean PHREAD score of at least. The file used to analyze the results was a FASTA file, and to transform FASTQ into FASTA, I used a PRINSEQ tool (83). The methylation status of each CpGs was checked by a pipeline software (Amplimethprofiler) that I developed in collaboration with a group of bioinformatics from my department. The pipeline is freely available at https://sourceforge.net/projects/amplimethprofiler (84). This tool is specifically designed for deep targeted bisulfite amplicon sequencing of multiple genomic regions and provides functions to demultiplex, filter and extract methylation profiles directly from FASTA files. In my analysis, all kind of filters were taken into account (read length, percentage of similarity between the end of the read and the primer sequence, bisulfite efficiency, maximum percentage of ambiguously aligned CG sites, percentage of aligned read). Using these filters, all reads that didn't match with expected length have been rejected. I used BLAST software (85) to aligned all reads to bisulphite reference of each gene in the analysis. As output, the pipeline returns: i) a summary and quality statistics file, containing information about the number of reads that pass filtering, the methylation percentage of each C in CpG sites, and the bisulfite efficiency for each C in non-CpG sites; ii) an alignment file where the bisulfite efficiency/read is calculated; iii) a CpG methylation profiles file, containing a matrix that reports the methylation status for each CpG dinucleotide: 0 if the site is recognized as unmethylated, 1 if the site is recognized as methylated, and 2 if the methylation state could not be assessed. Each row of the matrix can be considered as the CpG methylation profile and defines an epiallele in subsequent analyses. Then, we used this output to perform downstream analyses. Quantitative methylation averages for each site are then computed as the number of non-converted bases mapped on that site over the

total number of mapped reads. Single molecule CpG methylation arrangement was then performed. Based on R software (R Core Team, 2016, https://www.R-project.org), the abundance of each one of the 2NCpG distinct epialleles (where NCpG stands for the number of CpG sites in the analyzed region) was evaluated for each sample by counting the number of passing filter reads containing that epiallele. The filter was set in order to include only reads with the expected length and containing no more that 2% unconverted cytosine outside CpG sites.

3.8 Statistical analysis

In order to obtain a statistical significance for my data, I decided to use statistical tests suitable for each experiment. All statistical analyses were performed using JMP software (SAS, Cary, NC). Every time I showed a methylation average data, I expressed the results as means ± standard deviation. In all figure, the comparisons between 2 groups were performed using the unpaired Student t test, while for multiple comparisons were made by 1-way ANOVA followed by Tukey post-hoc test. For all average methylation data, a P-value ≤ 0.05 was considered statistically significant. For what concern the statistical analysis of epialleles results, I decided to correlate the epialleles distribution within each stages group using a Pearson correlation test. For this kind of analysis, a P-value ≤ 0.001 was considered statistically significant. A principal component analysis (PCA) was performed on the abundance of each 64 epialleles presents in the analyzed cell population. PC1 explained 31.2% and PC2 explained 29% of the observed variance. Beta diversity indicates the differences in epialleles assortment among groups and it assessed using " brain curtis distances"; this analysis is shown by principal coordinate analysis (PCoA) biplot that includes the impact of the 64 epialleles driving the samples clustering.

RESULTS

4.1 Candidate Gene

Using the latest technique in the field of sequencing, allowed me to study in a deep view the DNA methylation status of certain genes, I tried to better understand the mechanism underling the methylation generation. I used an innovative study, the epialleles approach, that allow to analyze the DNA methylation from a new point of view. To make the most of this technique, initially, I needed to find some strong changes in methylation average between different mice groups, in this way I was able to well define individual methylation profiles. First of all, I analyzed a large number of genes, that are involved in a correct development of mouse brain. Given the growing evidence of a strong correlation between mRNA levels and the methylation status of gene promoters, I decide to analyze the expression of genes involved in a brain development during the first days of embryonic growing and the firsts two months of life. In Figure 3A are shown the mRNA expression of some candidate genes, BDNF IV, CDKL5, Mecp2, Dlx5, FXYD1, DDO, FOX G1. As shown, the majority of these genes changes the expression levels during the early stages of mouse brain development. So, I proceeded to analyze the methylation status of the promoter of these genes. In Figure 3B are shown the methylation average for each gene, at different step point. The previous two figures highlight that there weren't correlations between methylation and expression for all genes. Among these, what appeared to be an increase in levels of expression in inverse proportion to the levels of methylation was *Ddo*. The increase of mRNA expression of this gene correspond to a strong demethylation of his promoter (30%) during early stages of development. This robust variation (the best of my analyzed genes), is the most important reason why I decided to use the *Ddo* as gene model for my studies.

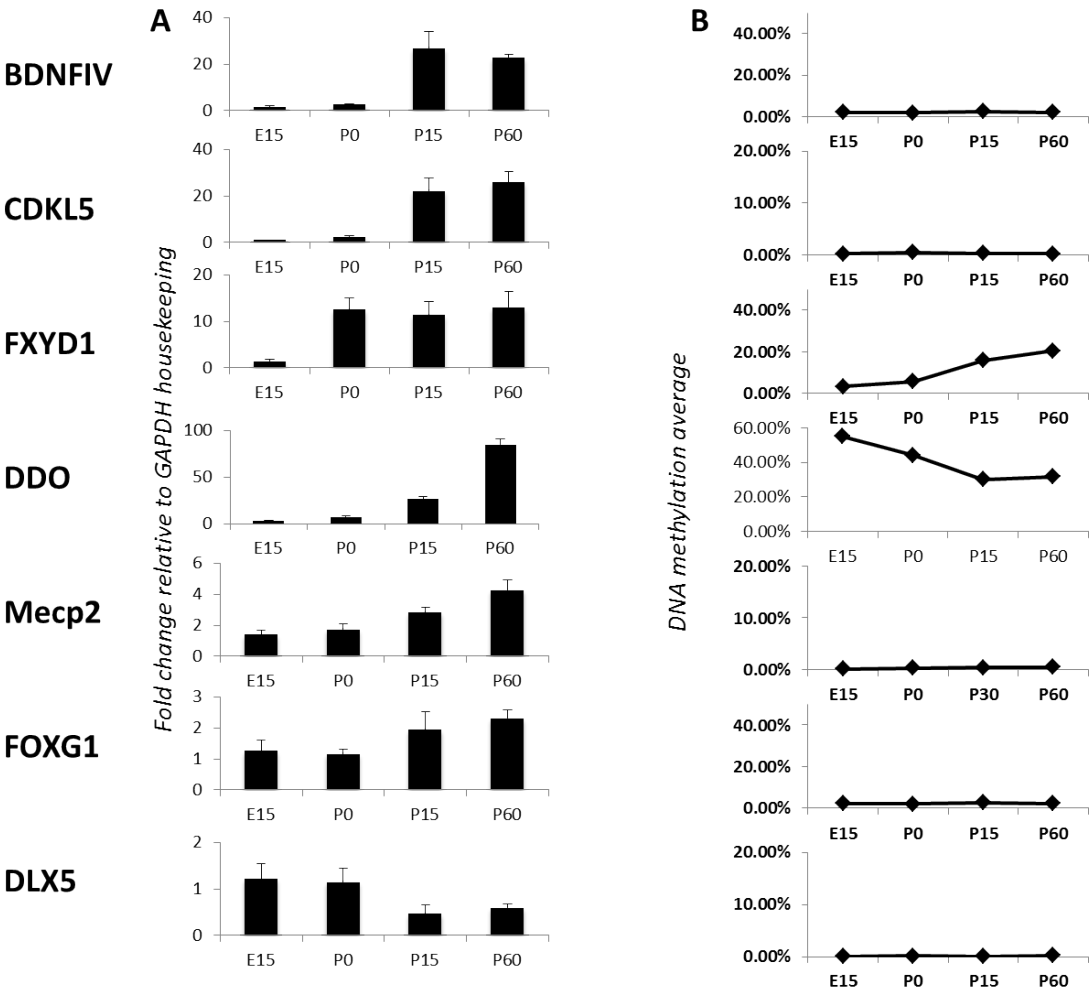

Figure 3. Candidate genes. A) The expression levels of BDNFIV, CDKL5, FXYD1, DDO, Mecp2, FOXG1, DLX5 genes. All experiments are normalized on the expression level of GAPDH. B) Average of methylation of the possible candidate genes.

4.2 Epialleles analysis principles

Amplicon bisulfite sequencing of a given genomic region enables us to determine whether each included CpG dinucleotide, in each single molecule, is methylated or unmethylated. Upon high-coverage bisulfite sequencing, it is possible to determine, with high precision, either the average methylation at each CpG site or the asset of methylated and unmethylated CpG sites present in each amplicon-derived sequence. As an example, a region that includes 4 CpG sites may give origin to 16 possible combinations that may be potentially found in a mixed population of cells (Fig. 4). These different combinations will be here referred to as epiallele; the number of different exhibited epialleles provides a measure of the level of epipolymorphism (see Figure 4 for details and examples). I applied this kind of methylation analysis to investigate the epiallele combinations and evolution of the *Ddo* gene, as example of a locus undergoing methylation changes during brain development.

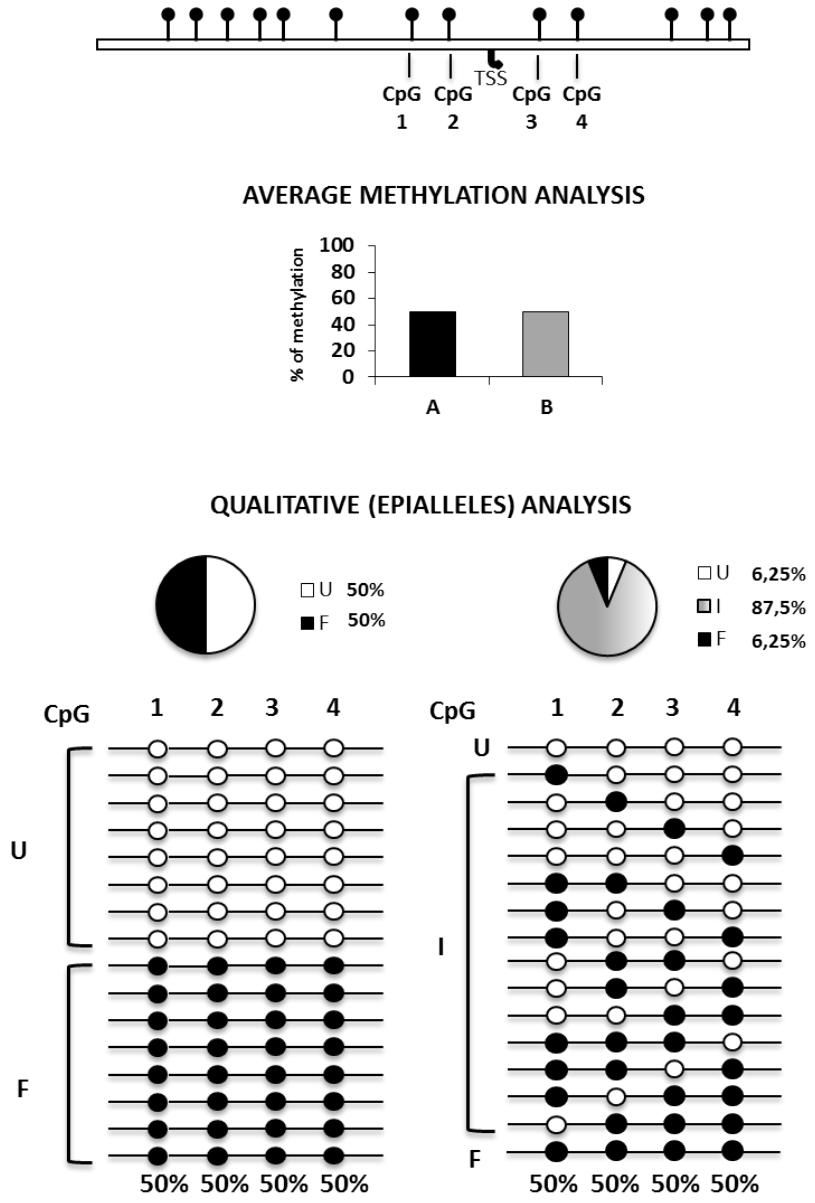

Figure 4. Principle of epipolymorphism and epiallele analysis. Averaged methylation degree, even at single base resolution, does not give any information on cell-to-cell methylation variability. In the example reported in the Figure, which shows analysis of 4 adjacent CpG sites, 50% methylation degree may correspond to completely different methylation scenarios. These range from the lowest degree of epipolymorphism (bottom left) to the highest level (bottom right). However, reliable analysis of the relative frequency of each epiallele must rely on a high number of analyzed sequences. Compared to genomic approaches previously used to measure the general epipolymorphism degree, the here adopted amplicon bisulfite sequencing, although limited to targeted genomic regions, allowed us to magnify the details of cell-to-cell epiallele variability at single loci, thanks of the very high sequencing coverage (about 210,000 in this study) and to comprehensively establish the methylation pattern of several adjacent CpG sites of longer regions (up to 600–1000 bp) in which all CpGs within individual reads are effectively phased and may represent the epigenetic haplotype. TSS: transcription start site. The pie charts represent the percentage of fully unmethylated epialleles (U = white), fully methylated epialleles (F = black), and the 14 remaining possible methyl CpG combination or intermediate epialleles (I = gray gradient). (From Florio et al 2017 Ref. 94)

4.3 Epialleles frequency distribution of Ddo during early stages of mouse brain development.

D-aspartate oxidase (*ddo*) is a FAD-containing enzyme that selectively deaminates bicarboxylic D-amino acids, such as D-aspartate (D-Asp), NMDA, and D-glutamate (86). In the Punzo et al. paper (76), were published the results about the mRNA expression and DNA demethylation average of *Ddo* during the early stages of mouse brain development. As said before, in my study I decided to deepen the generation of these DNA methylation variations, looking from another point of view, the epialleles analysis. First of all, I investigated 3kb of the promoter region of *Ddo* (3 mice for each stage, E15, P0, P30) in whole brain. The promoter of this gene (Fig. 5A) is poor in a number of CpGs and as shown in figure 5B the demethylation process that affected the region around TSS, is not common to all regions and to all CpGs. The first three regions (R1-R3) that aren't subject to a change in methylation average, while the R6 and R7 seem to undergo the same demethylation process of the regions R4 and R5, except for some CpGs. Then, I proceeded to do an epiallele analysis of all promoter regions of *Ddo*. The First regions analyzed was R4, in figure 6 are shown all possible epialleles of this region and their frequency at Stage E15. The results show that in the Region 4(that contains 6 CpGs) all possible theoretical epialleles (Sixty-four ($2^{6)}$) are present. The distribution of epialleles is not predictable, indeed at this stage, the fully methylated profile is around 13% (the average methylation was evaluated at about 56%), and the unmethylated molecules totaled about 10%, while the sum of intermediate epialleles is 77% but each of these is present in different percentage. The epialleles distributions among the mouse of the same stage and during the development are shown in figure 7. It's possible to note how the patterns were extraordinarily conserved among mice of same developmental stages (All statistical correlation, Pearson correlation, are showed in Tab 2). Moreover, during the development (E15 to P30), the percentage of Fullymethylated and Unmethylated epiallele strongly change, and the intermediated epialleles show a main shift from profiles with more methylated CpG (Tetra/pentamethylated) to those with less methylated (mono/dimethylated) (Fig. 6). The epiallele analysis was performed also for the other region of Ddo promoter and

for the minus strand of Region 4. The regions 1 to 3, as expected, don't show a changed in epialleles frequency, while the regions 5 to 7 (Fig. 8C), indicate strong changes as the region 4, but I still study these changes. The exploration of the lower strand (R4) (Fig. 8A, 8B), confirm two things: 1) the epialleles trend among different developmental stages; 2) the equal frequency distribution among the mice of the same age (data not shown). In order to confirm that the observed epialleles distribution obtained from my results is not random, I used a simulated analysis of epialleles distribution starting from the values of methylation average of each CpG in the region 4 (Fig. 9). As possible to understand from these results, the simulated epialleles distribution and the epialleles distribution of mice brain are strongly different. These results may indicate that the generation of methylation profiles is not random but it follows a precise scheme of formation and maintenance of DNA methylation.

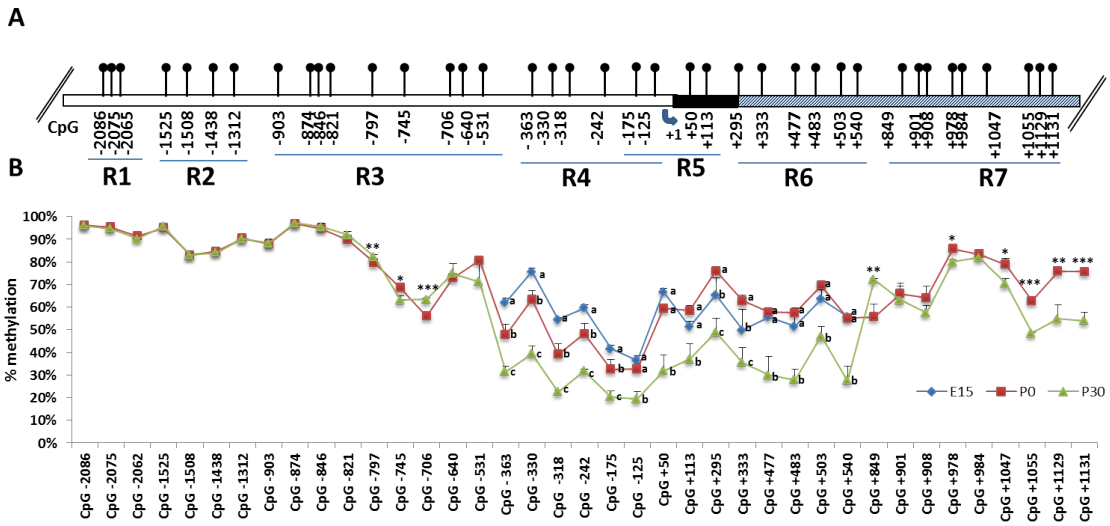

Figure 5. Quantitative methylation analysis of a 3 kb genomic region of Ddo gene. A) Structure of the putative mouse *Ddo* gene promoter. Blue arrow indicates the transcription start site (+1). White box represents the putative regulatory upstream region. Black box represents exon 1. Gray box represents first intron. Positions of CpG sites are indicated as relative to TSS. The analyzed 3 kb genomic portion is divided in 7 regions (R1-R2-R3-R4-R5-R6-R7) corresponding to different amplicons. B) Graph represents methylation average at each CpG site analyzed by Illumina MiSeq Sequencer. Each color line represents the average of 3 mice at a given developmental stage. Blue = E15; red = P0; green = P30. Error bars show standard deviations. For each CpG site, the points labeled with different letters on top are significantly different ($P < 0.05$) based on post-hoc ANOVA analysis (Tukey test, performed on each CpG site). Where two developmental times were considered, Student t test was applied with*$P < 0.05$, **$P < 0.01$, ***$P < 0.001$. (From Florio et al 2017 Ref. 94)

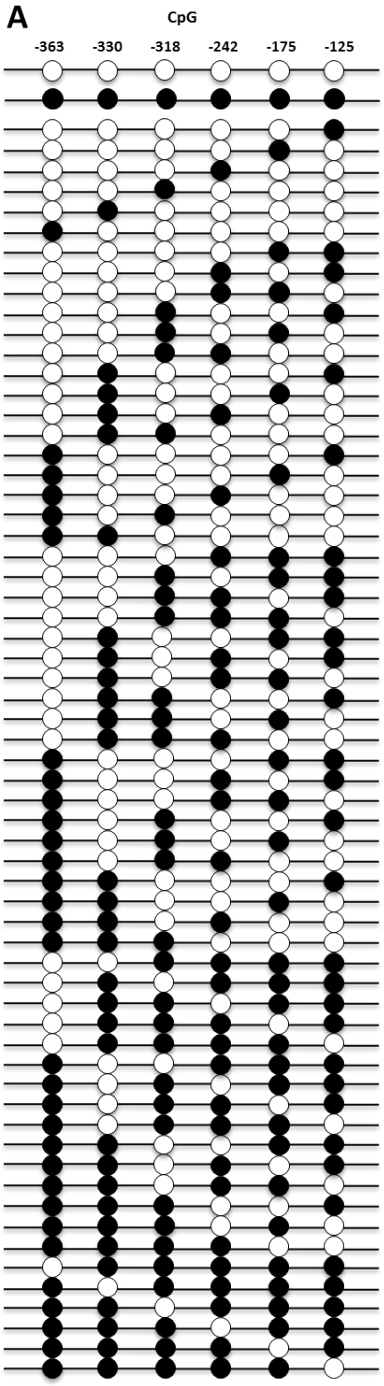

B

		E15		
		M1	M2	M3
U	UNMETHYLATED	9,9	10,2	8,6
F	FULLYMETHYLATED	10,9	15,7	13,7
1	-125	0,9	0,5	0,7
2	-175	1,3	0,8	0,8
3	-242	1,2	1,3	1,2
4	-318	0,3	0,4	0,3
5	-330	3,3	3,7	3,2
6	-363	1,8	1,6	2,2
7	-175-125	0,4	0,5	0,4
8	-242-125	0,4	0,3	0,3
9	-242-175	0,8	0,6	0,6
10	-318-125	0,1	0	0,1
11	-318-175	0,2	0,1	0,1
12	-318-242	0,3	0,2	0,3
13	-330-125	0,6	0,3	0,5
14	-330-175	0,8	0,8	0,8
15	-330-242	1,6	1,4	1,9
16	-330-318	1,7	1,3	1,6
17	-363-125	0,2	0,2	0,2
18	-363-175	0,5	0,4	0,4
19	-363-242	0,5	0,4	0,7
20	-363-318	0,3	0,4	0,4
21	-363-330	3	3,4	3,8
22	-242-175-125	0,6	0,4	0,7
23	-318-175-125	0,1	0,1	0
24	-318-242-125	0,2	0,1	0,1
25	-318-242-175	0,2	0,1	0,2
26	-330-175-125	0,4	0,4	0,3
27	-330-242-125	0,9	0,5	0,9
28	-330-242-175	1,1	1	1
29	-330-318-125	0,4	0,3	0,3
30	-330-318-175	0,7	0,6	0,6
31	-330-318-242	2	1,7	2
32	-363-175-125	0,2	0,1	0,2
33	-363-242-125	0,2	0,2	0,2
34	-363-242-175	0,5	0,3	0,4
35	-363-318-125	0,1	0,1	0,1
36	-363-318-175	0,1	0,2	0,1
37	-363-318-242	0,4	0,4	0,5
38	-363-330-125	0,6	0,7	0,7
39	-363-330-175	1,2	0,9	0,9
40	-363-330-242	2,6	2,7	2,9
41	-363-330-318	4,4	3,3	4,4
42	-318-242-175-125	0,2	0,2	0,2
43	-330-242-175-125	1,3	1,1	1,3
44	-330-318-175-125	0,6	0,6	0,6
45	-330-318-242-125	1,3	1,2	1,3
46	-330-318-242-175	1,9	1,6	1,8
47	-363-242-175-125	0,3	0,4	0,5
48	-363-318-175-125	0,1	0,1	0,1
49	-363-318-242-125	0,2	0,3	0,2
50	-363-318-242-175	0,5	0,3	0,3
51	-363-330-175-125	0,8	0,8	0,7
52	-363-330-242-125	1,3	1,4	1,3
53	-363-330-242-175	2,3	2,5	2,2
54	-363-330-318-125	1,1	1,2	1
55	-363-330-318-175	2,4	1,8	1,9
56	-363-330-318-242	7,7	7,1	7,3
57	-330-318-242-175-125	2,3	2,3	2,6
58	-363-318-242-175-125	0,6	0,4	0,5
59	-363-330-242-175-125	2,8	3,4	2,7
60	-363-330-318-175-125	1,7	2,1	1,8
61	-363-330-318-242-125	5,1	4,8	4,8
62	-363-330-318-242-175	7,7	8	7,6

Figure 6. All possible methyl CpG combinations (epialleles) at the Ddo R4 region. A) Representation of all 64 theoretically possible epialleles at region R4 of Ddo promoter containing 6 CpG sites. Circles represent the CpG sites analyzed (-363, -330, -318, -242, -175, and -125); black circles = methylated CpG; white circles = unmethylated CpG. B) Percent frequency of each epiallele in whole brain from 3 mice (M1, M2, and M3) at E15 stage. (From Florio et al 2017 Ref. 94)

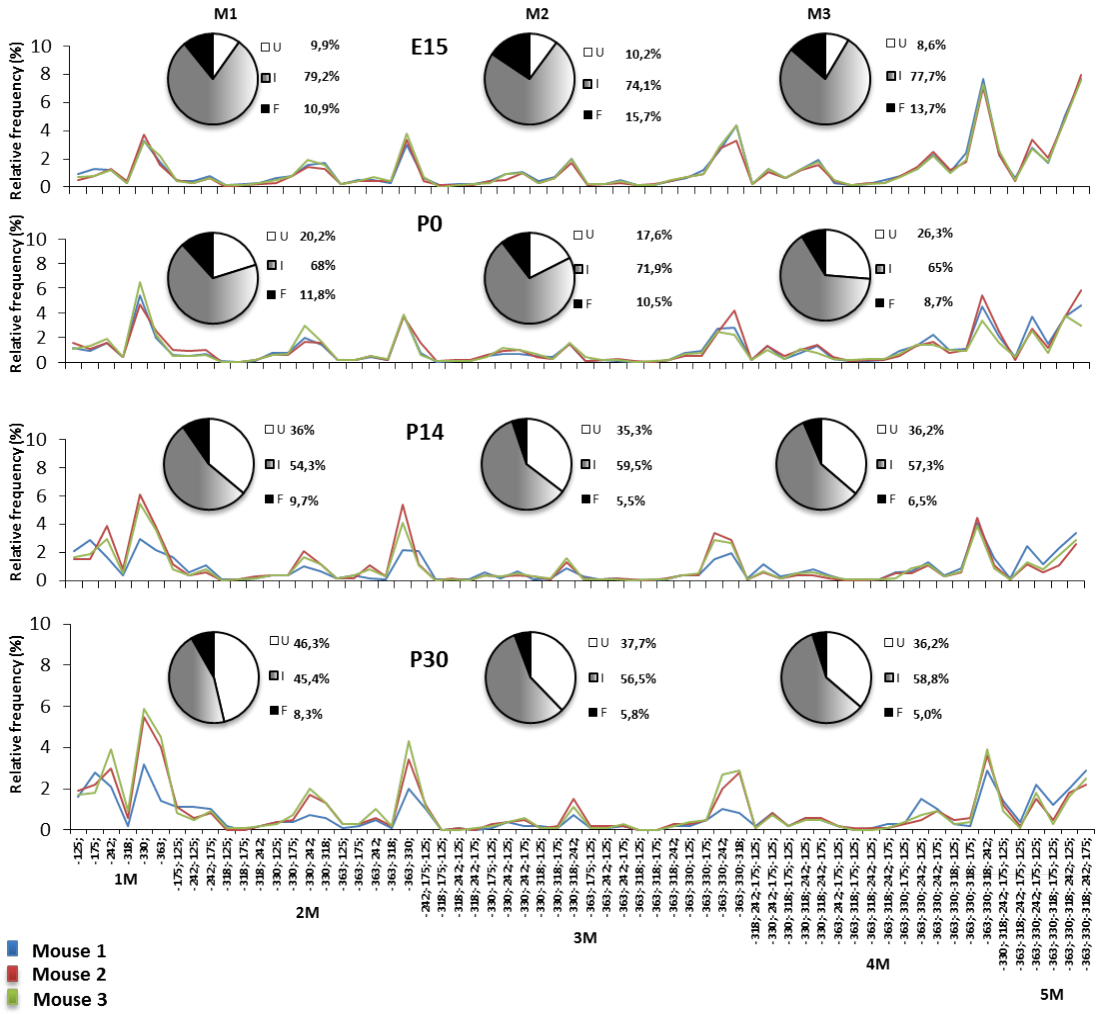

Figure 7. Epialleles frequency distribution at *Ddo* R4 region during different stages of mouse development (E15, P0, P14, P30). The pie charts represent the percentage of unmethylated epialleles (U = white), fully methylated epialleles (F = black), and all 62 intermediate epialleles (I = gray gradient). The line graph shows the percentage of each of the intermediate epialleles; each color line identifies one mouse. Blue = mouse 1; red = mouse 2, green = mouse 3. At the bottom of the last graph, the specific methyl CpG combinations of the 62 intermediate epialleles are reported. 1M identifies the group of monomethylated molecules; 2M = dimethylated; 3M = trimethylated; 4M = tetramethylated; 5M = pentamethylated epialleles. Pearson correlation R reported in Table 2. (From Florio et al 2017 Ref. 94)

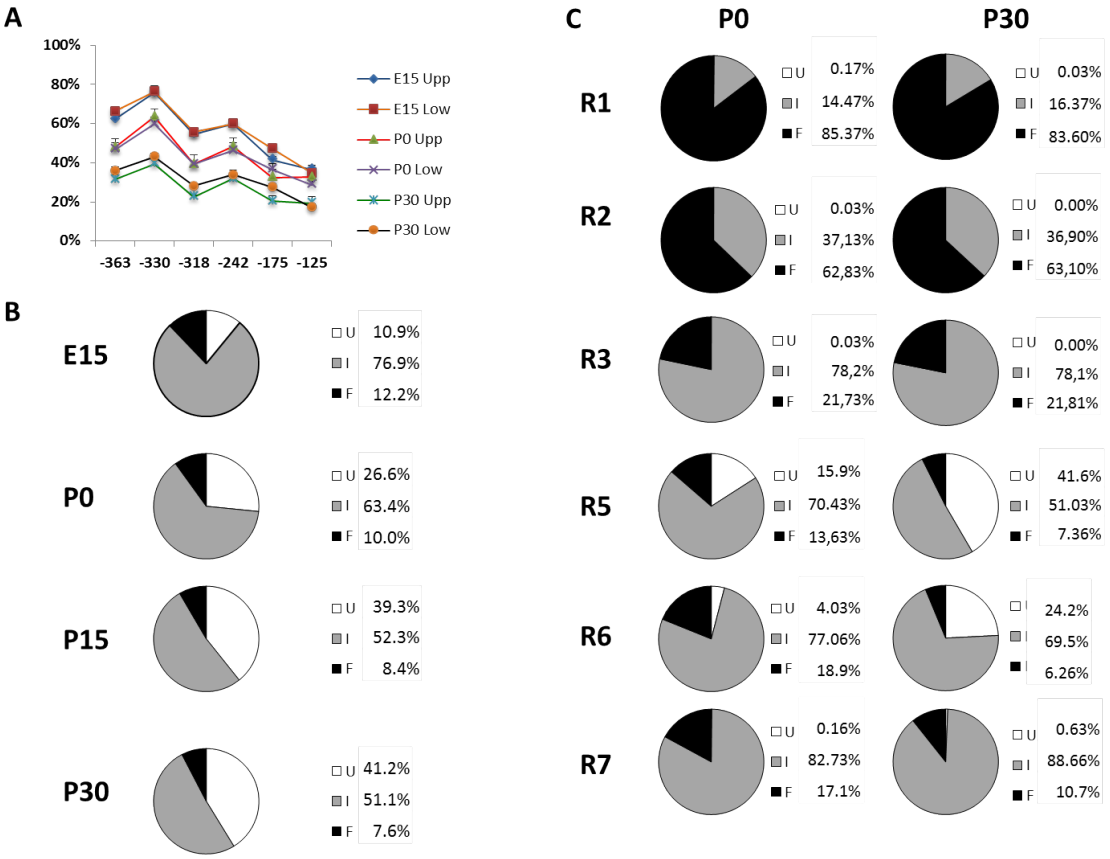

Figure 8. A) Comparison between upper and lower strand methylation average of R4 *DDO* promoter region. B) *DDO* R4 Lower strand Epialleles distribution during four early stages of mouse development(E15-P0-P15-P30). C) Ddo promoter (R1-R2-R3-R5-R6-R7) epialleles evolution from P0 to P30 stages.The pie charts represent the percentage of unmethylated epialleles (U = white), fully methylated epialleles (F = black), and all intermediate epialleles (I = gray gradient).

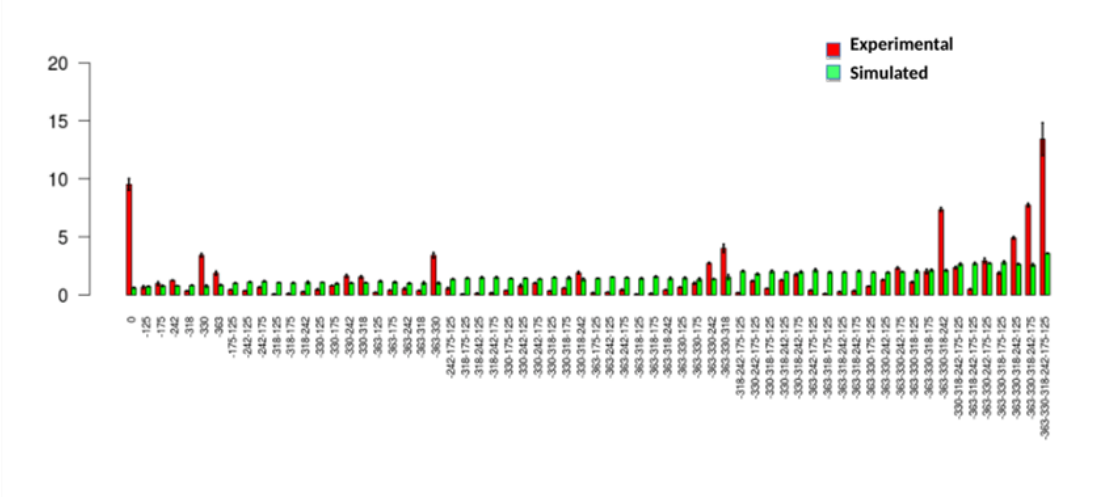

Figure 9 Simulation approach showing how the observed epiallele frequency deviates from the random distribution. The results for three representative samples (whole brain at E15 developmental stage) are reported. Similar conclusions were reached also for all the other data points considered in this study (data not shown). A bootstrap/simulation approach was performed in the following way: to obtain a synthetic dataset of 10000 molecules, each containing 6 CpG sites, we first generated an array of 10000 x 6 cells filled with zeros. Then, to simulate stochastic methylation events, one cell was selected in an iterative and random manner by substituting its zero value with 1. The cycle was stopped when the global methylation probability (57% in the case of E15 whole brain) from the observed data was reached. This procedure was repeated three times in order to mirror the three mice used in the study. Briefly, the same methylation probability was assumed for all CpG sites (1/n, where n is the number of CpG sites). The frequency of each simulated epiallele was averaged and compared it with the real observed frequency. The results are shown in the barplot. On x-axis the epialleles and on y- axis their frequencies are reported, respectively. Red bars: real epiallele frequency; green bars: simulated epiallele frequency. The error bar of each observed epiallele in no case intersects with that of the corresponding simulation, indicating that the experimentally observed epiallele distribution was not random. (From Florio et al 2017 Ref. 94)

Table 2.

Pearson correlation test of epialleles distribution *Ddo* R4 region			
STAGE	**Mice**	**Pearson R**	**p-value**
E15	M1/M2	0,986067197	1,89637E-48
E15	M1/M3	0,992391755	2,71669E-56
E15	M2/M3	0,9868598	3,30893E-49
P0	M1/M2	0,959438583	1,08587E-34
P0	M1/M3	0,944346038	1,15656E-30
P0	M2/M3	0,88145423	3,27535E-21
P14	M1/M2	0,786309702	3,66001E-14
P14	M1/M3	0,846990179	4,13024E-18
P14	M2/M3	0,981271547	1,26582E-44
P30	M1/M2	0,833321788	4,37257E-17
P30	M1/M3	0,801413887	5,13155E-15
P30	M2/M3	0,984769846	2,69114E-47

4.4 The epialleles configuration of brain areas.

To better understand if the epialleles distribution of whole mouse brain is equal in all brain areas or if there is a specific distribution for each of these, I performed the epialleles analysis of Ddo promoter Region 4, in five different brain areas (hippocampus HIPP, cortex CX, prefrontal cortex PFC, cerebellum CB, and striatum ST)at P30 age. Before this, I have assessed the methylation average of each area and then of all single CpGs (Fig. 10A and 10B). Three areas (CX, PFC, CB) seem to have a similar value, while the Hippocampus area and Striatum area show respectively low(15%) and high levels(50%) of DNA methylation. For what concern the epiallele analysis (Fig. 10C), first of all, is possible to note the different percentage of unmethylated and fullymethylated epialleles among different areas (Fig. 10C). Especially the striatum shows no more than 30% fullymethylated epiallele compared to the methylation average of 50% of this area. In the same way, the percentage of fullymethylated epiallele in the Hippocampus area is around 2%, while the methylation average is around 18%. Moreover, the intermediate epialleles distribution is highly heterogeneity among the brain areas. Notably, the difference among the areas often fall on the same methylation profiles, that are always present in each area but with different percentage (see peaks in the Fig. 10C.).

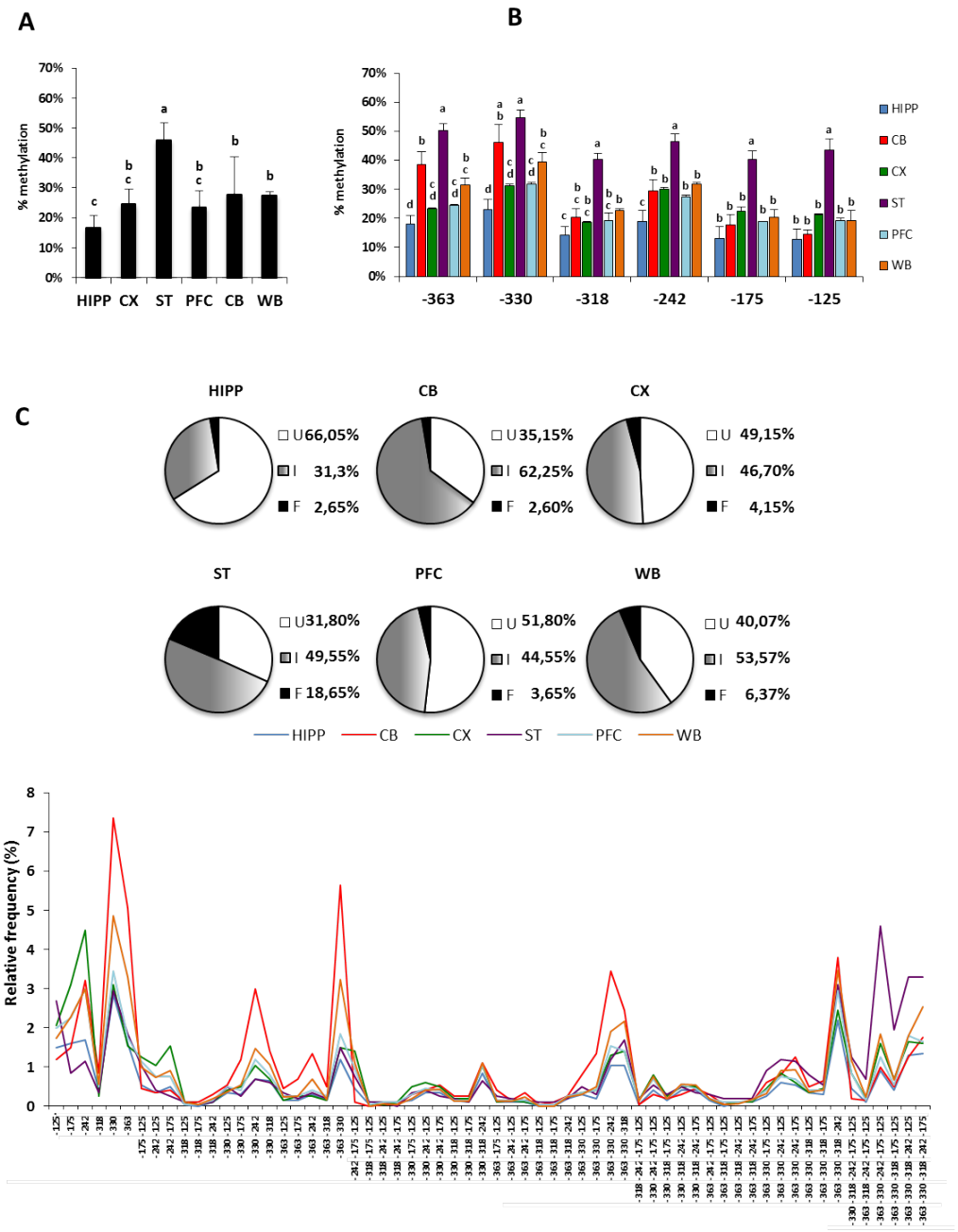

Figure 10. Epialleles composition analysis of *Ddo* R4 in separated areas of mouse brain (Hipp: hippocampus; CB: cerebellum; CX: Cortex; ST: striatum; PFC: prefrontal cortex) and in whole brain (WB) at P30 stage. A) Average methylation at the *Ddo* R4 region in each separated brain area. The bars labeled with different letters on top are significantly different based on post-hoc ANOVA statistical analysis (Tukey test). B) Average methylation at each CpG site (-363, -330, -318, -242, -175, and -125). The bars labeled with different letters on top are significantly different based on post-hoc ANOVA analysis (Tukey test) performed for each CpG site. C) *Ddo* R4 region epiallele frequency distribution. The pie charts represent the percentage of unmethylated epialleles (U = white); fully methylated epialleles (F = black); and all 62 intermediate epialleles (I = gray gradient). Each color line represents the distribution of 62 intermediate epialleles in one brain area, as indicated. At the bottom of the graph, the specific methyl CpG combinations of each of the 62 intermediate epialleles are reported. A P-value < 0.05 was considered statistically significant. (From Florio et al 2017 Ref. 94)

4.5 Neural cells population analysis reveals a specific epialleles distribution.

Once analyzed the epialleles frequencies in mouse whole, noted that there is a different distribution among the brain areas, I decided to investigate the methylation status of neuronal cells to understand if the high degree of epipolymorphism of brain tissue may be explained by the cellular heterogeneity. To do this, I analyzed four diverse neuronal cells population: neurons, oligodendrocytes, astrocytes, and microglial The first step was to investigate the average of methylation of the region 4 of Ddo promoter in these cells. As shown in Figure 11A the average of methylation isn't too far among populations, except for astrocytes cells that exhibit a much lower percentage. The microglial seems to have slightly higher levels of methylation than other cells. Then I performed an epialleles analysis (Fig. 11B), and the results indicate that the population with a low level of methylation (astrocytes) shows a high presence of unmethylated, monomethylated and dimethylated epialleles; while the higher methylated population shows an high frequency of tetramethylated and pentamethylated epialleles. One more time, as in the whole brain and in brain areas samples, the differences among the cell population always are due to the same CpG combinations. In particular, there are some epialleles that are constantly present, and they born from specific CpGs: -363, -330, -242. These sites seem to be more susceptible to methylation processes, conversely the sites -175 and -125 appear to be more resistant to the methylation event. All the results derived from brain tissue and from neuronal cells suggest that there is a scheme in which a specific chain command indicate the cytosine able (or not) to undergo a methylation processes. In summary, we confirmed that most of the methylation rules observed in brain tissues are applied also for isolated brain cells, including the high percentage of intermediate epialleles, high degree of epipolymorphism, and high conservation of epialleles frequency among the same type of cells among individuals. These important rules seem to highlight that the methylation processes could be happened in a deterministic way rather than in a stochastic manner.

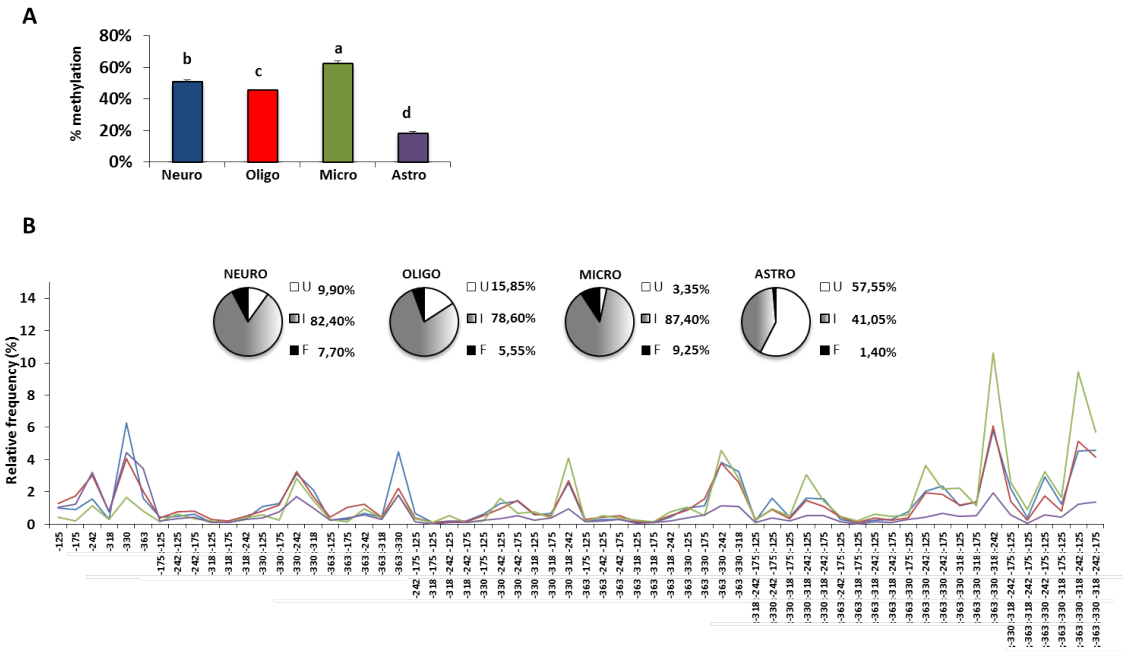

Figure 11. Averaged and single molecule methylation analysis of the *Ddo* promoter region in isolated primary brain cells A) Average methylation in different indicated brain cells. The bars labeled with different letters on top are significantly different based on post-hoc ANOVA statistical analysis (Tukey test). B) Frequency distribution of intermediate epialleles in primary cells. Neuro: primary neurons, blue bars in A and blue lines in B. Oligo: primary oligodendrocytes, red bars in A and red lines in B. Micro: primary microglial cells, green bars in A and green lines in B. Astro: primary astrocytes cells, violet bars in A and violet lines in B. in A (bars) and C (lines). The pie charts represent the percentage of unmethylated epialleles (U = white); fully methylated epialleles (F = black); and all 62 intermediate epialleles (I = gray gradient). At the bottom of each graph, the specific methyl CpG combinations of each of the 62 intermediate epialleles are reported. (adapted from Florio et al 2017 Ref. 94)

4.6 Clonal feature of immortalized cell line

Given the previous results, I wanted to understand if the same epialleles configuration studied in neuron and glia cells may be kept in an immortalized neuronal cell line. For this reason, I performed the methylation analysis using two different plates of A1 cells(c-myc immortalized neurons). In figure 12A it is possible to see that the methylation average of these two cell plates as well as being similar to each other, is also similar to the primary neuron cell line (compare to figure 11B). This result lets believe that the epialleles frequencies could be similar, but unexpectedly the A1 cells shown a completely random distribution (Fig. 12B.) with an enrichment of few

epialleles and the total absence of others. Moreover, the configuration of methylation profiles is absolutely discordant between the two plates of immortalized neuron (Pearson R = 0.083). The lowest degree of epipolymorphism suggests that the immortalized neuron may be able to acquire a kind of clonal-like behavior, probably influenced by stochastic events.

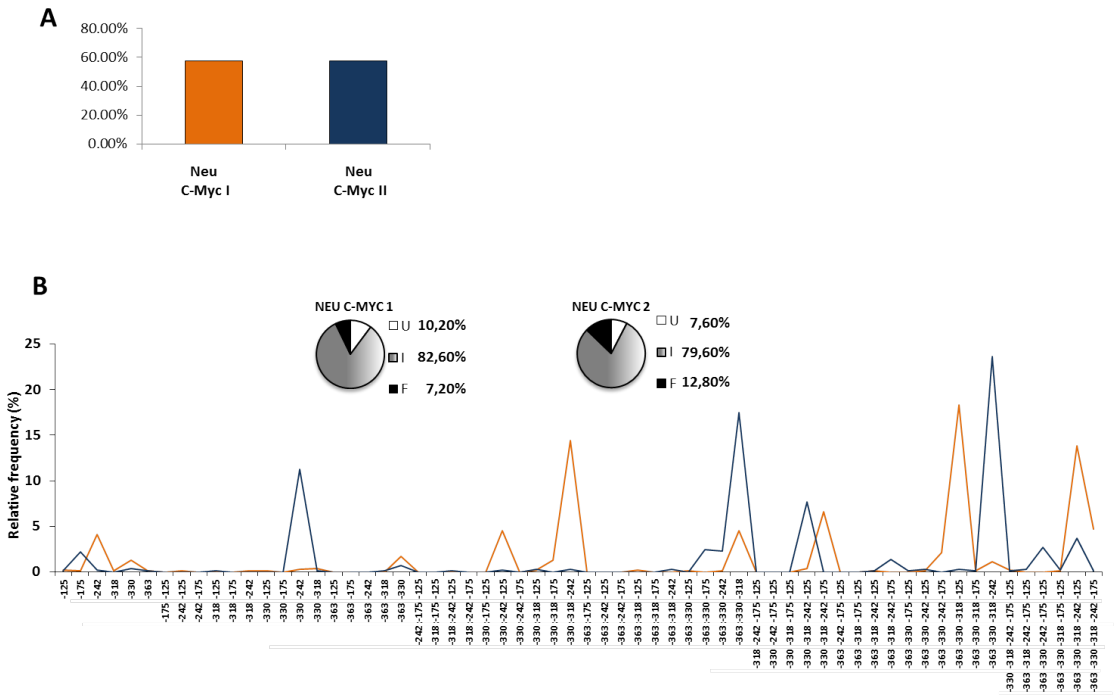

Figure 12. Averaged and single molecule methylation analysis of the *Ddo* promoter region in cultured c-myc immortalized neurons. A) Average methylation. B) Epiallele distribution in c-myc cultured immortalized neurons. Neu C-Myc I and Neu C-Myc II: A1 C-Myc immortalized neurons, dark blue and orange, respectively, in A (bars) and B(lines). The pie charts represent the percentage of unmethylated epialleles (U = white); fully methylated epialleles (F = black); and all 62 intermediate epialleles (I = gray gradient). At the bottom of the graph, the specific methyl CpG combinations of each of the 62 intermediate epialleles are reported. (Adapted from Florio et al 2017 Ref. 94)

4.7 From embryonic stem cells to neural cells

Which is the origin of frequently methylation profiles that are present in all different neural cell populations? To answer this question, I evaluated the epialleles distribution of *Ddo* region 4 in a model of neural cells differentiation derived from stem cells (ESCs). This is one of the most surprising results, indeed, despite the similar methylation

average of these CpGs (Fig. 13A and 13B), the epialleles frequency shows a different configuration in these two kinds of cells (Fig. 13C). At the step of Embryonal stem cell, the distribution appears like a random way, where only the monomethyl epialleles seem to be slightly high. On the other hand, when the ESCs differentiate, appears a specific reorganization of each epiallele; it seem that during differentiation process, from a random state, the cells pass through a tidy state (Fig. 13D). One more time there is a prevalence of few peaks against others; indeed during differentiation, the epialleles that contain a -242 and/or -125 (and their derivate) decreases, conversely the epialleles derivate from -330 and -363 undergo a substantial increase. These results even more in a clear manner, suggest that behind the methylation or demethylation processes there is a precise deterministic mechanism that decides the destiny of each single CpG. Additionally, the epialleles distribution of differentiated stem cells strongly looks like a neuron or glial epialleles distribution; the peaks that rise in a chart (Fig. 13D) match to the majors seven epialleles detected in developing whole brain as well as neurons and glial cells, with different relative abundance. These seven epialleles are: -330; -363; -330/-318; -363/-330; -363/-330/-318; 363/-330/-318/-242, 363/-330/-318/-242/-175. As possible to note, there is a strong presence of -330 and -363 CpGs, that influences the idea of the existence of methylated sites that are better able to guide the methylation process of near CpGs. For this reason, the figure 14A shows the heat maps of each CpG contribution to form all epiallele kind in four cell population (ESC, nESC, neuron, astrocyte). It is easy to note how the heat maps of ESC is significantly different from other populations, while the latter three are very similar to each other.

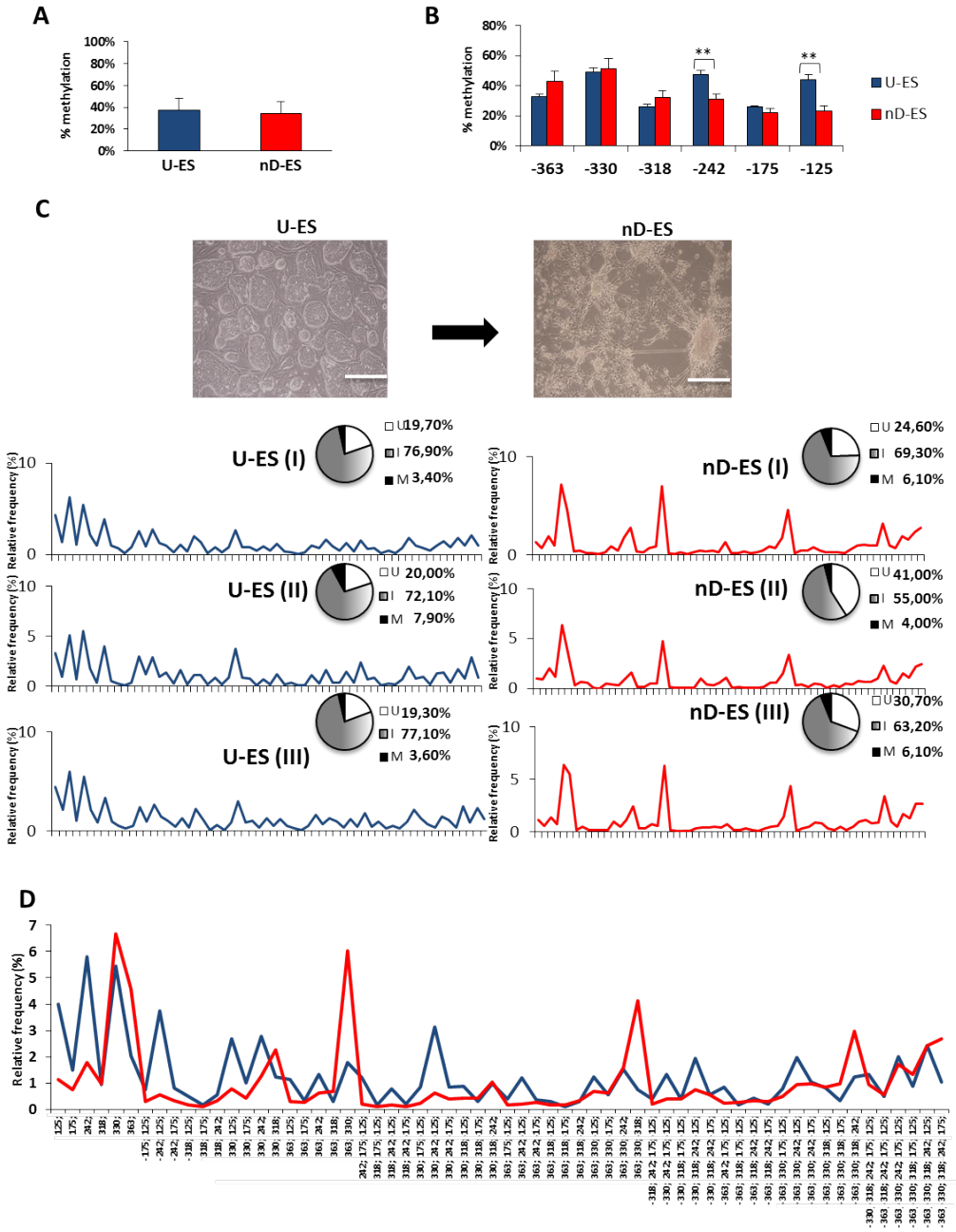

Figure 13. Single molecule methylation analysis in ESC neural differentiation model. A) Averaged methylation at *Ddo* R4 region in undifferentiated ESCs (U-ES) and in differentiated ESCs (nD-ES) from 3 independent experiments. B) Averaged methylation of each CpG site (-363, -330, -318, -242, -175, and -125) at Ddo R4 region (data are showed as mean +/-standard deviation; **P < 0.01). C) Microscope images of ESCs in undifferentiated state (U-ES) and upon differentiation toward neuronal phenotype (nD-ES). Bar =200 mm. Epiallele frequency distribution in 3 independent ESCs differentiation experiments (I, II, and III). The pie charts represent the relative percentage of fully unmethylated epialleles (U = white), fully methylated epialleles (M = black), and the 62 intermediate epialleles (I = gray gradient). The line plots represent the frequency distribution of each of the 62 intermediate epialleles (blue: undifferentiated ESC; red: differentiated ESCs). D) Comparison between average frequency distribution of each of the 62 Ddo intermediate epialleles, from 3 independent experiments, in undifferentiated (blue line) vs. differentiated (red line) ESCs. The specific methyl CpG combinations of each of the 62 intermediate epialleles are indicated on the x-axis.

4.8 Principal Component Analysis of neural cell and ESC

Another interesting point regard a post-hoc analysis based on epialleles frequency of all single cell population. Using a Principal Component analysis, I tried to perform an epigenetic correlation among all kind of neural cells analyzed in this work. The correlation was established on the abundance of each epiallele in each cell line. In figure 14B there are two graphs in which there is respectively the location of each cell population and of each epiallele. In the first graph it is important to note how the embryonal stem cells are located almost equidistant from the other population. Conversely, the neural population differentiated from ESC is positioned closely to neuron and astrocyte cells. In the second graph it should be noted the influence of monomethyl epiallele containing the CpG -363 and -330 [5,6] that are displayed in the same part where are located astrocyte, neuron and n-ES cells, to remark the importance of these CpG in these cells; while the monomethyl epialleles that contain the CpG -242, -175 and -125 [1,2,3] are much closer to ESC. Therefore it seems more truthful the assumption that in undifferentiated cells the methylation events occur randomly, while in differentiated cells the methylation /demethylation processes may follow a precise schedule, where the methylated state of more susceptible sites increases the likelihood that adjacent resistant sites become methylated.

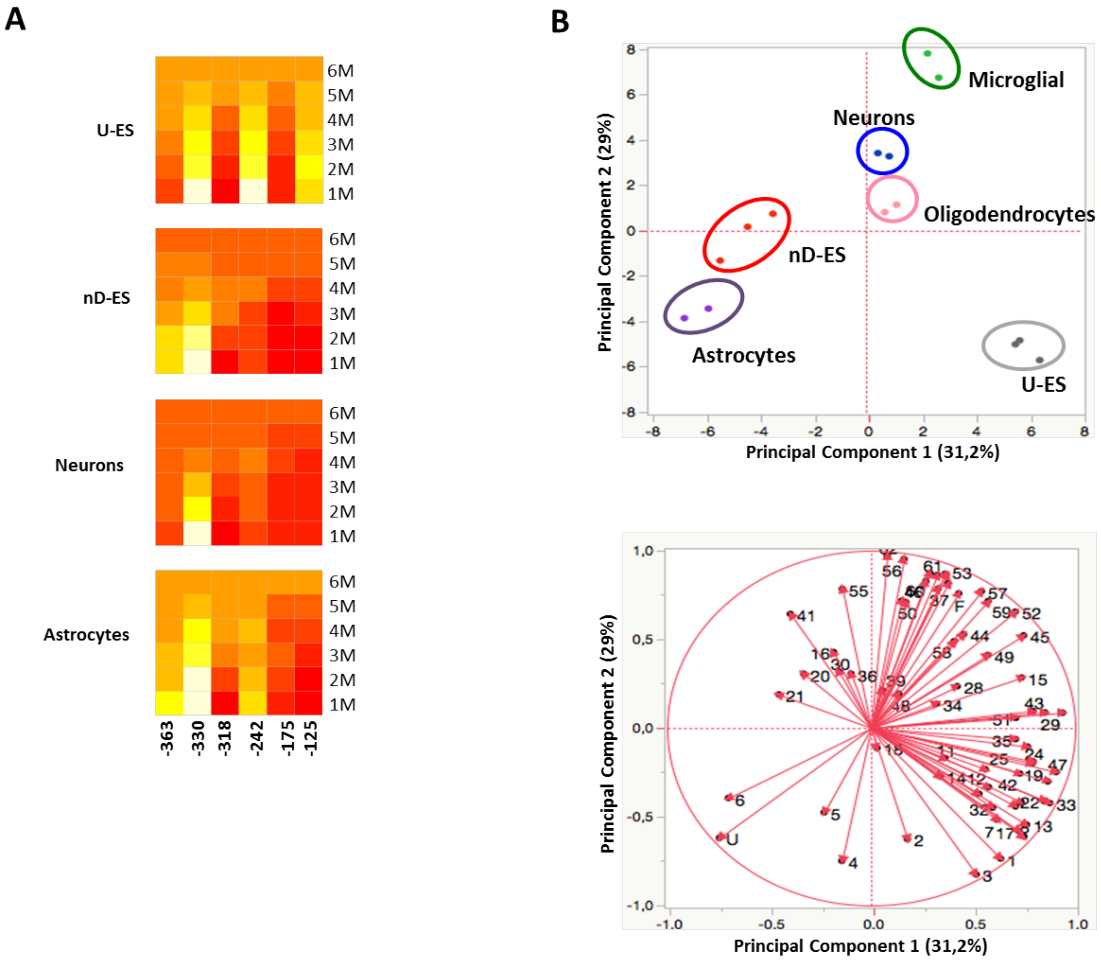

Figure 14 A) The heatmaps show the contribution of each CpG in different epiallelic classes among 4 cell types (U-ES = undifferentiated ESC; nD_ES = neuronal differentiated ESCs). The color scale from red to yellow (from low to high values) shows the contribution of each CpG to formation of monomethylated (1M), dimethylated (2M), trimethylated (3M), tetramethylated (4M), pentamethylated (5M), and fully methylated (6M) molecules, respectively. B) Epigenetic correlation of Ddo R4 epialleles distribution in ES and different purified brain-derived cell types performed by PCA. Scores plot represents the distribution of each specific cell type (blue = neurons; pink = oligodendrocytes; green = microglial; violet = astrocytes; gray = U-ES undifferentiated ESCs, red = nD-ES differentiated ESCs). The analysis was based on the qualitative and quantitative influence of each of the 64 epialleles displayed by each cell type. In the Loading plots of PCA the vectors represented by red arrows show how (the direction) and how much (the length) each epiallelic profile contributes to the individual correlations represented by PC1 and PC2. Note that each epiallele is named with numbers (1–62) or letters (U, F), as reported in Fig. 6

4.9 Dynamic evolution of DDO lower strand epialleles during neural differentiation.

As above showed, the epialleles distribution between upper and lower strand of DDO promoter region follows the same demethylation process during the early stages of mouse development. For this reason, I decided to investigate the methylation status of

DNA lower strand during neural differentiation starting from ES cells (day 0) and passing through the days 2, 4, 8, up to day 14 of differentiation (mature neuron). As shown in figure 15, during the neural maturation the methylation average undergoes a significant increase until day 8 then sugnificantly decreased, returning at final stages (day 14) to a similar percentage of day 0. These results are in agreement with data previously shown about the methylation of DDO Upper strand in stem cells. The evolution of epiallele distribution during these differentiation events follows a specific dynamic that it was unexpected. Indeed, the epialleles conformation at embryo stem cell level (day 0) (Fig.16) seems to be equally distributed with two major peaks: the fully un-methylated and fully methylated profiles. Instead, at days 2 and 4 it was possible to appreciate a strong shift toward the penta-methylated and fully methylated profiles (Fig. 17 A and B), where especially the fully methylated profile reaches a 50% at day 4. Surprisingly, between day 8 (Fig. 18) and 14 (Fig. 19) the epialleles frequency distribution underwent a significant variation, since the number of more methylated epialleles strongly decreased while the fully unmethylated profile peaked up to 20%. During these changes, the intermediate epialleles were shaped in an ordered manner and showed a distribution strongly resembling the adult mouse brain profiles. To better understand if there is a specific correlation between epialleles distribution and each stage of neural differentiation, I performed a “betadiversity” analysis. In figure 20 the PCoA plot represents the beta diversity and shows a specific epialleles assortment in each group, where each differentiated stage cluster away from others. These results suggest the existence of a well orchestrated mechanism that generates and dynamically modulates the frequency of each epiallele during the neural differentiation from day 0 to day 14.

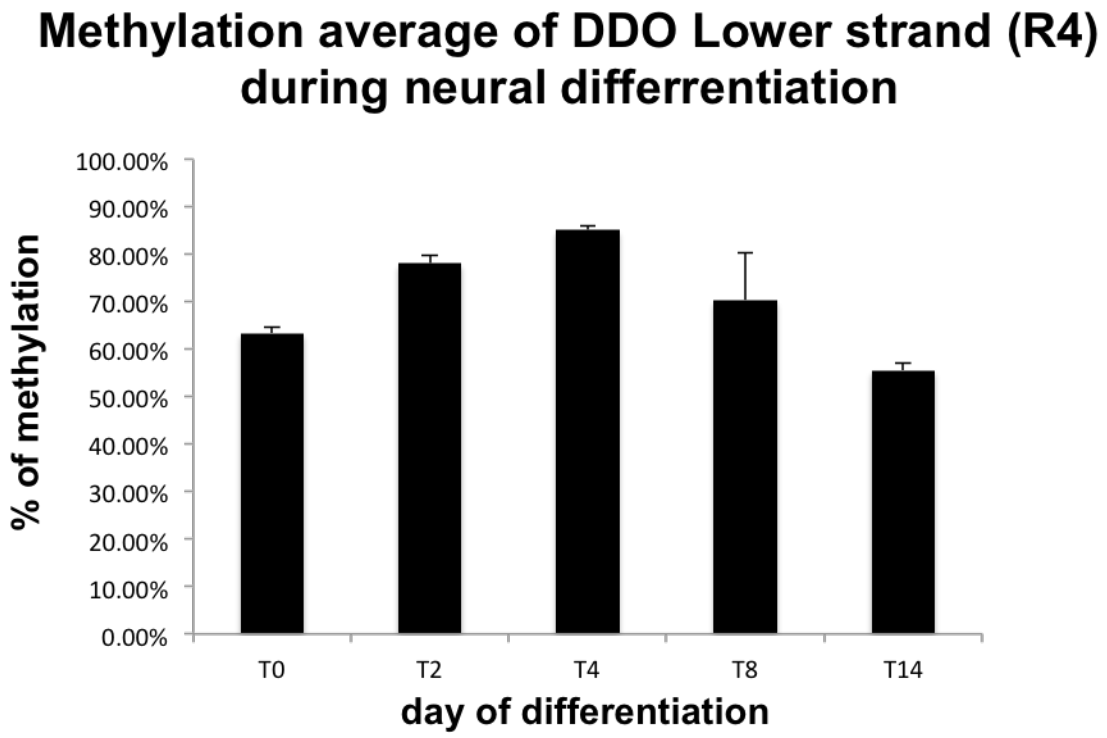

Figure 15. The methylation average of DDO R4 lower strand during the neural differentiation from embryo stage (day 0) to day 14. Each bar represents one stage of differentiation.

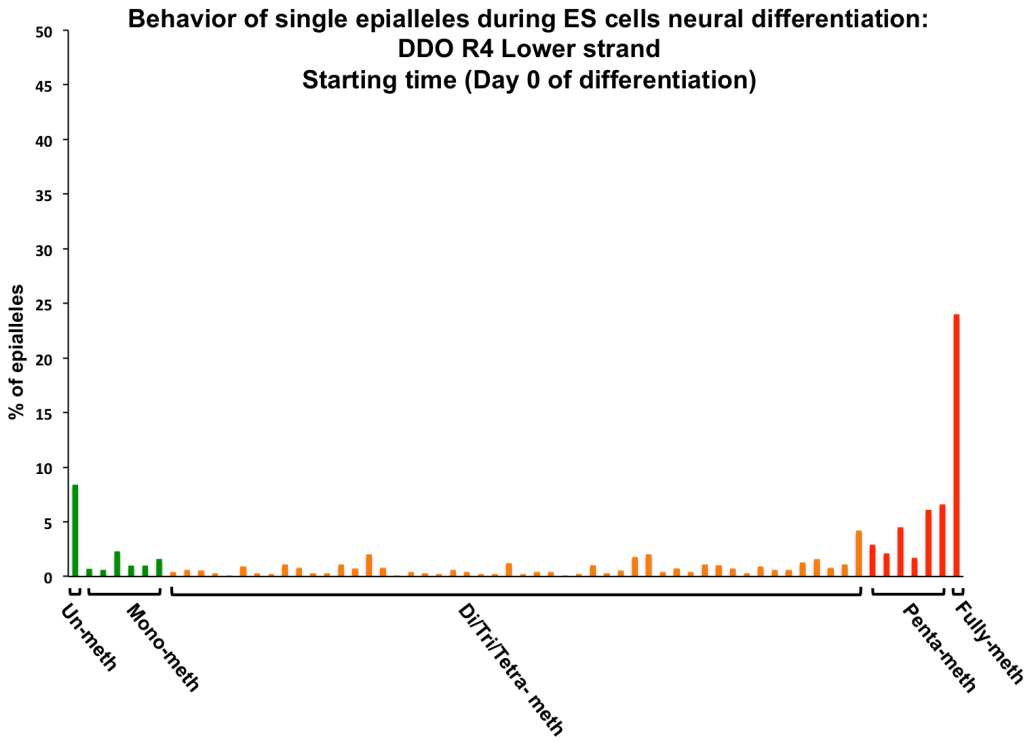

Figure 16. The epialleles distribution of DDO R4 lower strand at embryo stage (day 0). On the x axis is report the seven epialleles classes: un-methylated and mono-methylated (green), di-methylated, tri-methylated and tetra-methylated (orange), penta-methylated and fully methylated (red). The y-axis represents the percentage of each epiallele at this stage of differentiation.

A

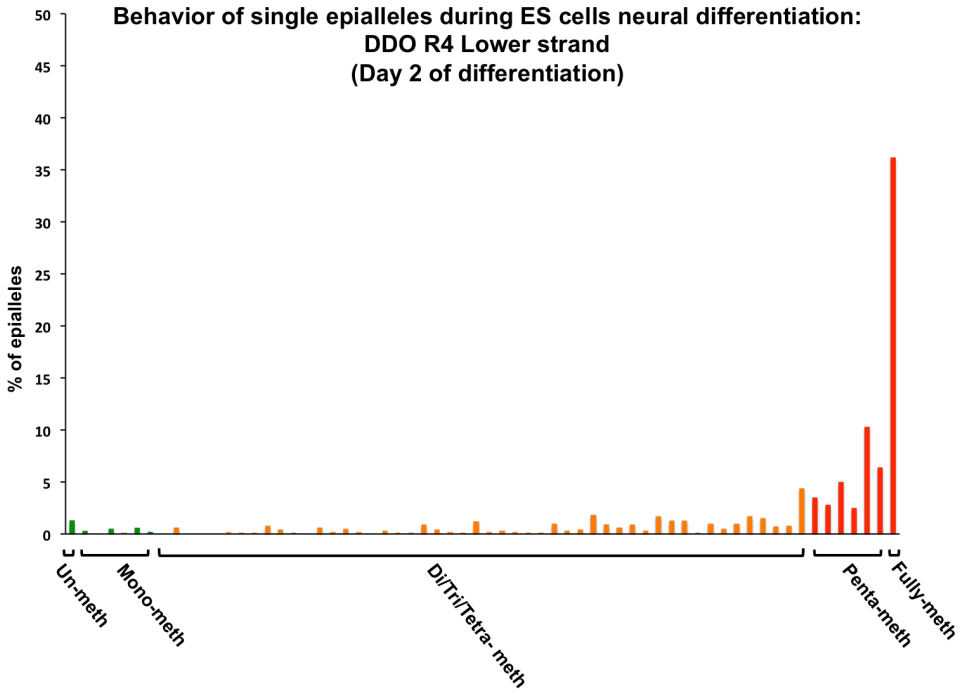

B

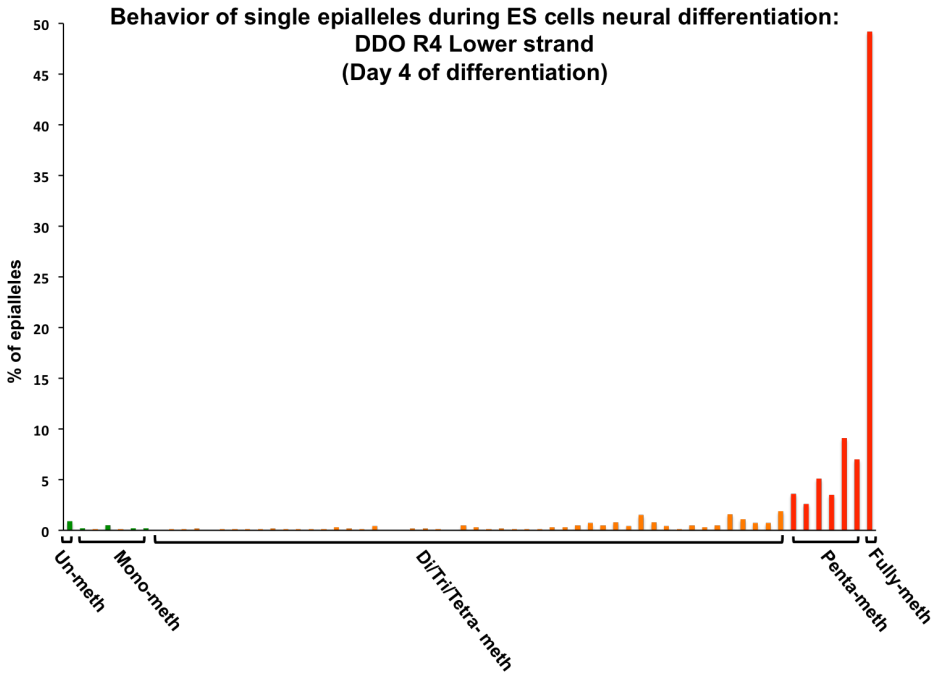

Figure 17. The epialleles distribution of DDO R4 lower strand at day 2 of neural differentiation (A) and at day 4 (B). On the x axis is report the seven epialleles classes: un-methylated and mono-methylated (green), di-methylated, tri-methylated and tetra-methylated (orange), penta-methylated and fully methylated (red). The y-axis represents the percentage of each epiallele at this stage of differentiation.

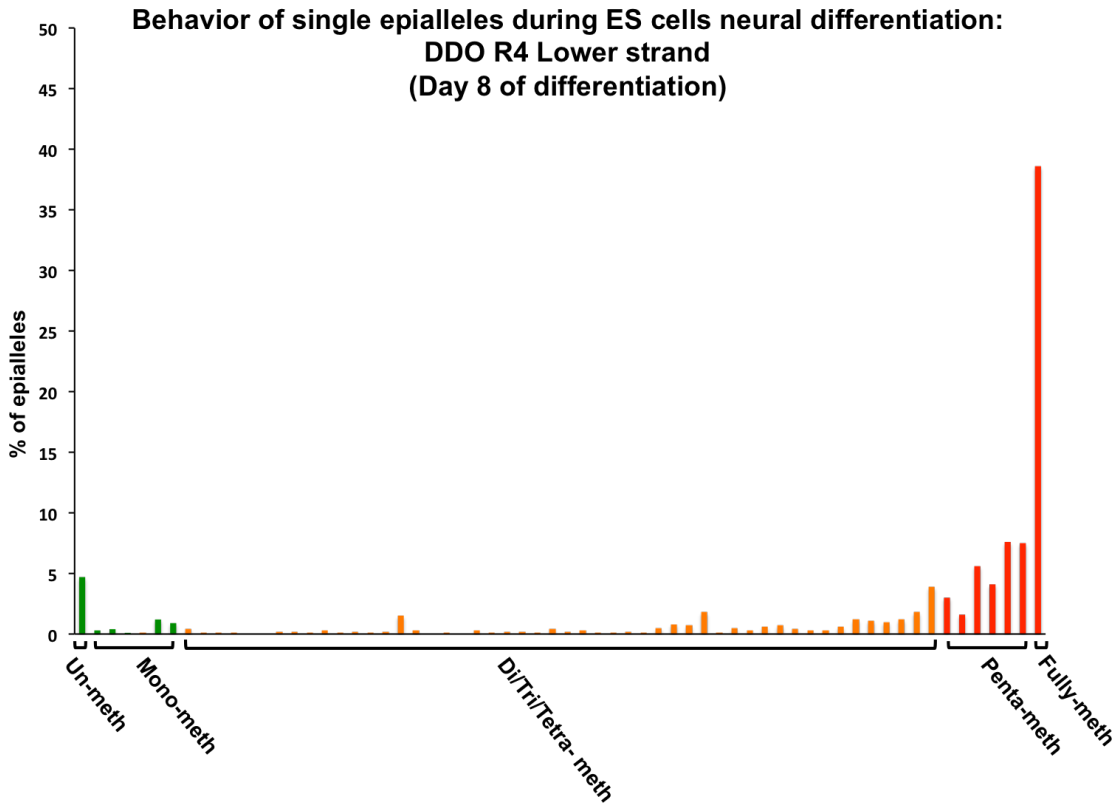

Figure 18. The epialleles distribution of DDO R4 lower strand at day 8 of neural differentiation. On the x axis is report the seven epialleles classes: un-methylated and mono-methylated (green), di-methylated, tri-methylated and tetra-methylated (orange), penta-methylated and fully methylated (red). The y-axis represents the percentage of each epiallele at this stage of differentiation.

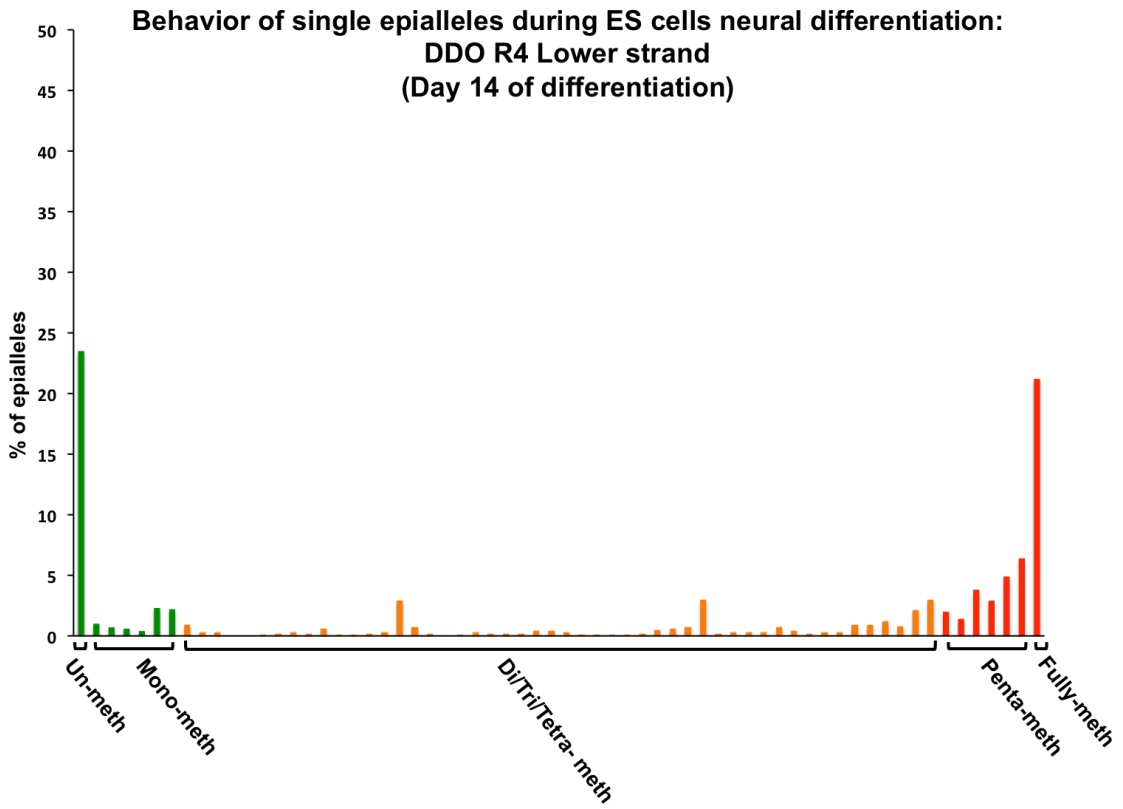

Figure 19. The epialleles distribution of DDO R4 lower strand at day 14 of neural differentiation. On the x axis is report the seven epialleles classes: un-methylated and mono-methylated (green), di-methylated, tri-methylated and tetra-methylated (orange), penta-methylated and fully methylated (red). The y-axis represents the percentage of each epiallele at this stage of differentiation.

The beta diversity analysis of DDO R4 Lower strand during neural differentiation

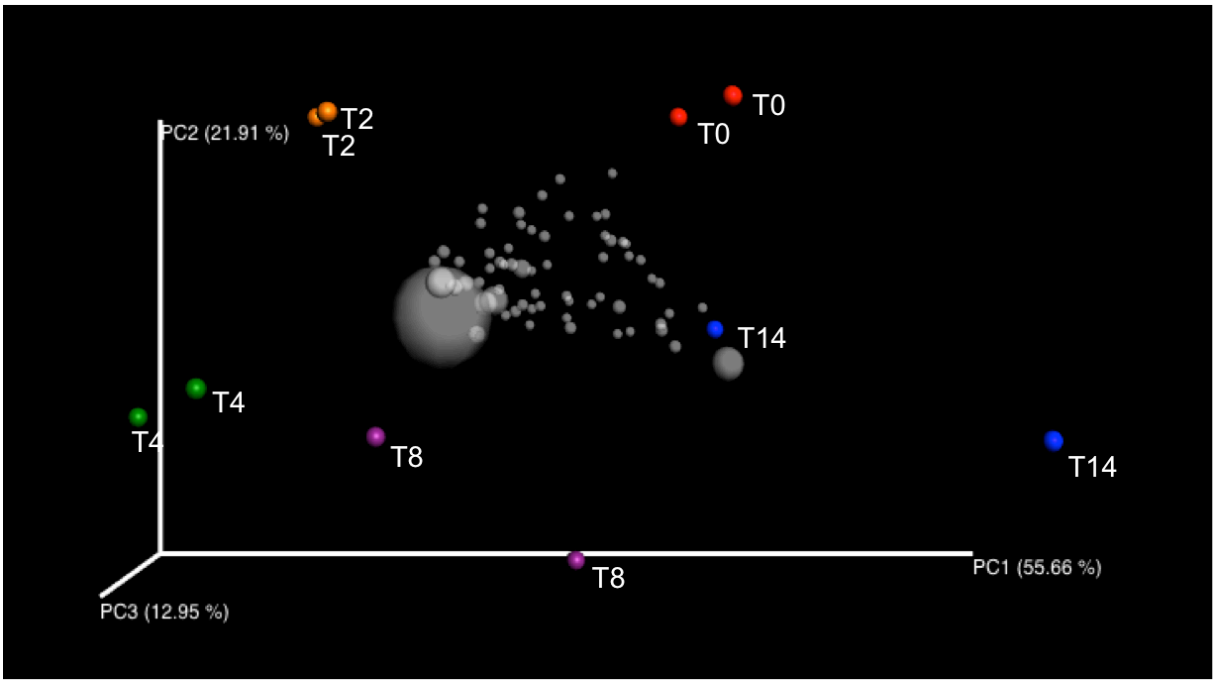

Figure 20. The PCoA plot of beta-diversity analisys performed on DDO R4 lower strand epialleles distribution during the neural differentiation from ES cells. The colored circles represent each stage of neural differentiation (red = day 0, orange = day 2, green = day 4, violet = day 8 and blue = day 14). The gray circiles represent the 64 possible epialleles, The dimension of gray circles represents the abundance of each epiallele.

4.10 Dynamic evolution of Nanog, BDNF, tubulin III and GFAP expression and methylation during neural differentiation.

I sought to determine the variation of DNA methylation profiles of genes involved in neural and glial differentiation to check whether they are affected by changes similar to the above considered reference gene. In most of cases I found that methylation profiles (Fig. 21) changed consistently and inversely correlating with the expression profiles (not shown) making these genes additional and functionally appropriate ideal models to study the role of epiallele distribution variation during differentiation. Indeed, ongoing chromatin immunoprecipitation experiments in my lab are trying to elucidate the factors involved and the mechanisms underlying the changes in epiallele distribution during differentiation and to study independently the methylation and demethylation processes. Finally, about the general meaning of the epiallele distribution during differentiation and development, in our lab we are currently trying to translate these findings to human brain and brain cells in order to check whether anomalies in epialleles profiles generation and maintenance may be associated with neuropsychiatric conditions.

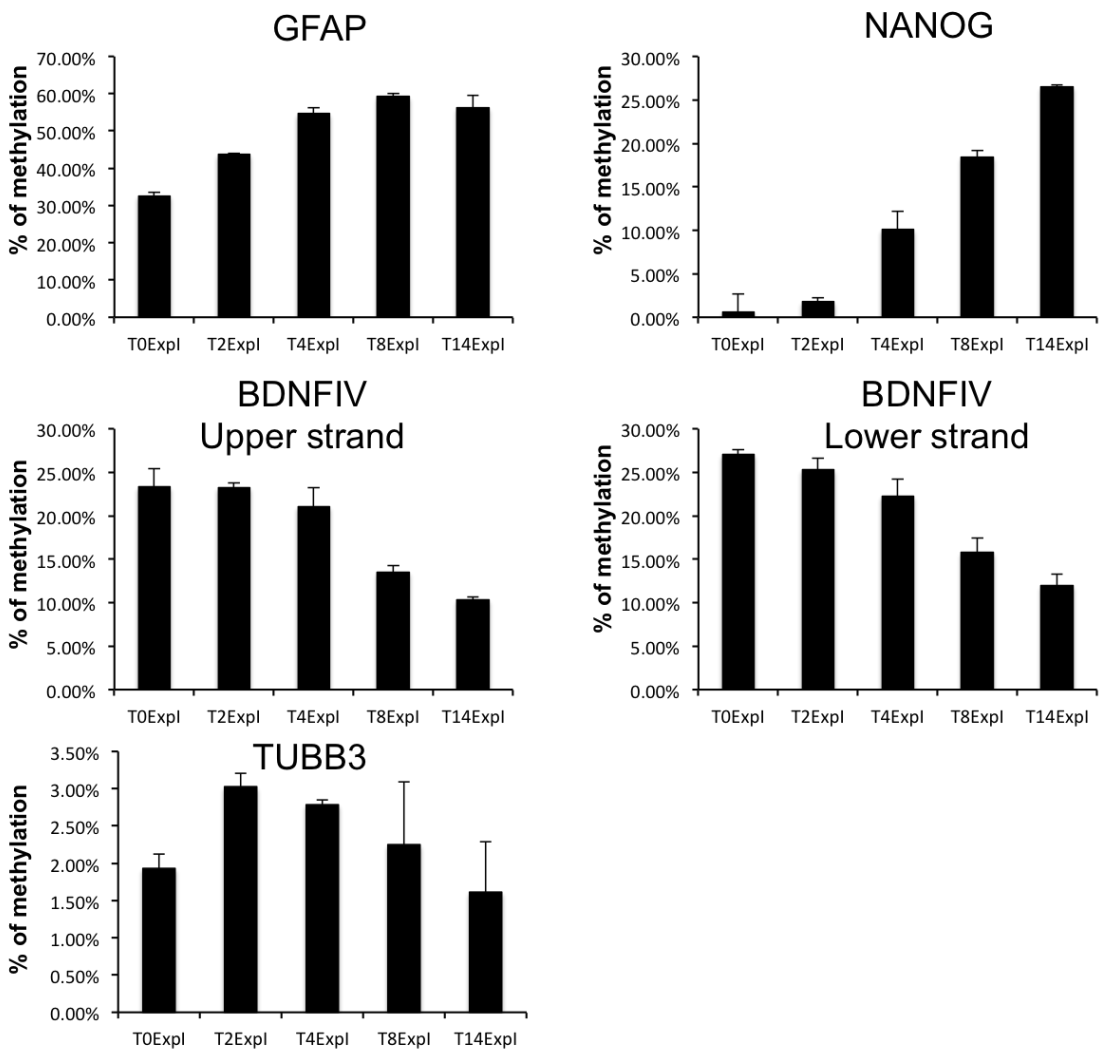

Figure 21. The methylation average of genes implicated in neural differentiation (Nanog, BDNFIV Upper and lower strand, Tubuline III and GFAP. The methylation average is evaluated during neural differentiation from embryo stage (day 0) to day 14. Each bar represents one stage of differentiation (day 0, day 2, day 4, day 8, day 14).

DISCUSSION

5.1

Several studies addressing DNA methylation patterns at genomic level in health and disease, have successfully identified tissue- or disease-specific DNA methylation patterns and differentially methylated regions during normal development or in diseased states (28-30, 48, 68, 69, 71, 87). However, the great majority of these studies, even when performed at high resolution, could measure the average CpG methylation at each locus while the processes driving methylation establishment and changes are still poorly understood. In this study, I have performed an ultra-deep methylation analysis to study the methylation profiles of single genomic regions (surrounding *Ddo* gene) taking into account the cell to cell heterogeneity and quantifying the frequency of each methylation pattern (epiallele) present in mixed and pure populations of brain cells during development and neural differentiation. The results substantiate well appreciated general phenomena including: i) high degree of epipolymorphism is detected either in whole brain, in brain areas and in isolated brain cells, being virtually all combinations of methylated CpGs represented at variable frequency; ii) the majority of epialleles were neither fully methylated or fully protected in all the analyzed systems; iii) the relative epiallele frequency distribution changed during development, it was different among individual brain areas, as well as in different purified brain derived cells, but profiles were always strikingly conserved among individual developmental stages, brain areas or primary cell types derived from different mice; iv) cultured neurons transformed by c-myc showed lower degree of epipolymorphism and stochastic epiallele enrichment showing profiles strongly divergent among different cell plates and passages; v) an epigenetic drift at *Ddo* gene, clearly appreciated in term of epiallele profiles and fully unpredictable by conventional methylation determination, marked ES cells neural differentiation process. Overall, the finding of strong conservation in the epigenetic diversity and epialleles frequency distribution, also in purified cells, supports the possible existence of mechanisms oriented to maintain the epigenetic system in a dynamic stability, where the methylation state of each CpG in single cells is not stable

rather it is subject to periodic fluctuations. In particular, results obtained by differentiating ESC suggest that in the undifferentiated state the different CpG sites are methylated independently and stochastically while a well-orchestrated interplay between contiguous CpGs differing in methylation susceptibility underlies specific epiallele frequency and dynamics in differentiated state. This appears to occur in a spatial-specific manner where the methylated state of more susceptible sites (e.g. -330 and -363 in the R4 region) favour methylation of adjacent otherwise partially resistant sites. These rules are retained in mature brain where the differential average methylation in each cell type mainly derives by the relative percentage of fully methylated and unmethylated molecules and by the relative abundance of specific peaks, (including mono-, di- tri-, tetra- and penta-methylated molecules, respectively) within a prevalent fixed set of intermediate epialleles. Whether these rules may apply to different genomic regions, are limited to some specific regions (e.g. CpG poor promoter) or are a peculiarity of *Ddo* promoter, remains to be determined. However, I believe that my data represent a solid proof of concept that epialleles analysis, possibly implemented by studies on set of genes, and using mutant mice and disease-model, may reveal unprecedented mechanism underlying DNA methylation establishment, dynamics and alteration within tissue cell populations. The present study clearly demonstrates the importance of single molecule methylation analysis in mixed, as well in pure, cell populations and points on the informativeness of epiallele frequency distribution analysis, to be eventually associated to evaluation of average methylation, in order to get insight into the origin of methylation heterogeneity and, possibly in the near future, its functional relevance. Although the limit of this approach is that it does not allow one to directly match cell by cell methylation, mRNA expression and cell identity data, this approach may circumvent the difficulties and the high costs of the single-cell analysis with which it shares the ability to investigate in detail cell to cell methylation differences in a cell population. We have recently developed a pipeline, namely amplimethprophiler (https://sourceforge.net/projects/amplimethprofiler), that render such kind of analysis, performed at individual genomic loci, easily approachable by other researchers interested to apply these principles to any biological system and genomic regions. At our knowledge, nowadays no studies have addressed the epialleles

diversity in brain and in brain-derived cells. In the recent past, very few studies ingeniously addressed the cell to cell methylation heterogeneity, prevalently in tumor systems and at genome-wide level (74, 75, 88-91), supporting general rules that are mostly consistent with the here presented data. Landan and colleagues (75) suggested that a stochastic series of subtle and progressive methylation changes in cancer evolution leads to deterministic methylation profiles. A spatially specific methylation patterns emerged, by means that some CpGs are particularly sensitive to changes in methylation creating an initiation point for methylation that then spreads over the region. Our data are compatible with this model according which in subsets of cells within each population, methylation profiles take origin by the spreading from susceptible sites that when methylated become able to influence nearby CpGs. Moreover, by the reanalysis of RRBS data from normal and cancerous tissues, Landan et al. (75) also observed that two methylation patterns of DNA molecules from the same cell population are rather different each with other with exception of H1 ESC and testis which displayed coherent and homogeneous methylation profiles. By contrast, in developing brain and purified brain cells we found a striking conservation of epiallele profiles at *Ddo* gene within the same type of samples deriving from different mice. Moreover, we found that in undifferentiated ES cells the methylation profiles were rather disorganized and highly polymorphic at *Ddo* gene shifting toward an ordered, non-stochastic and less polymorphic epiallele profile upon induction of neural differentiation. These apparent discrepancies may derive by the fact that our analysis was based on a much higher number of reads per locus and that it was performed on CpG poor gene regulatory region that may behave in a different and more specific manner compared to CpG rich regions which are mostly considered, especially in RRBS-based analyses, by genome wide approaches. Indeed it has been demonstrated that in physiological conditions CpG poor promoters are subjected to a much finer methylation-dependent control compared to dense CpG regions (7, 92). In a recent study, Li et al. (74), using the methclone program, were able to map a series of loci (eloci), consisting in 4 adjacent CpGs, subjected to epigenetic drift during leukemia progression. This study, based on combinatorial entropy as a measure of epialleles shift observed at single loci throughout the genome, revealed enrichment of eloci in the

genic region, in particular at promoter regions, which is in line with my findings. Moreover, by the analysis of eloci during leukemia progression, the authors concluded that the analysis of epiallele composition may reveal clonal shifts at specific loci otherwise not detectable. In agreement with this observation, I found that, upon differentiation of ES cells, *Ddo* promoter underwent a methylation shift, as clearly detected by epiallele analysis, which was unpredictable by traditional methylation analysis. However, previous studies addressing epialleles composition were mostly performed in tumor progression systems, and thus epialleles changes were interpreted as clonal shifts. It would be very interesting in the future to establish whether the epigenetic drift, here reported at *Ddo* gene during differentiation, is due to a clonal effect or, rather and more likely, to a methylation remodelling occurring in ES cell population upon induction to differentiate.

CONCLUSION

6.1

My studies highlight how the new way (epialleles analysis) to study the DNA methylation may reveal some changes in methylation status of certain genes difficult to find by classical approach. Leveraging an ultra-deep sequencing method, the epialleles analysis, allowed me to better characterize the methylation status of *Ddo* promoter during the mouse brain development and in neural differentiation starting from embryonic stem cell. The obtained results show that in brain tissue there is a high polymorphic methylation that may undergo to a constant turnover. Moreover, the extraordinary degree of conservation among mice with the same stage of development, among the same types of cell populations indicate that the generation of methylation profiles seems to be dictated by an accurate mechanism governed by a deterministic principle. These rules, may not be valid in immortal cells (like tumoral cells), where the apparent clonal behavior does underpin possible stochastic influences. In addition, the epigenetic drift that occur during neuronal differentiation from stem cells, visible only using epialleles technique, strengthens the hypothesis that there are unambiguous methylation mechanisms underlying neuronal development. Moreover, my results evidenced a pyramidal epiallele hierarchy. In a few words, if one CpG is methylated there is a higher probability that the adjacent CpG will be methylated. Overall, given that my findings indicate that epialleles composition dynamics in brain cell population is very finely tuned and strikingly conserved, I conclude that tracking epiallele profiles may help “to identify barcodes” to get insight into mechanisms underlying DNA methylation establishment, changes and, potentially, alterations of these processes in neurodevelopmental diseases that may be not revealed by conventional, either gene specific or genome-wide, averaged methylation analyses.

REFERENCES

1. Jaenisch R, Bird A. *Epigenetic regulation of gene expression: how the genomeintegrates intrinsic and environmental signals*. Nat Genet. 2003 Mar;33 Suppl:245-54. Review. PubMed PMID: 12610534.

2. Goldberg AD, Allis CD, Bernstein E. Epigenetics: a landscape takes shape. Cell. 2007 Feb 23;128(4):635-8. Review. PubMed PMID: 17320500.

3. Quina AS, Buschbeck M, Di Croce L. *Chromatin structure and epigenetics.* Biochem Pharmacol. 2006 Nov 30;72(11):1563-9. Review. PubMed PMID: 16836980.

4. Strahl BD, Allis CD. *The language of covalent histone modifications*. Nature.2000 Jan 6;403(6765):41-5. PubMed PMID: 10638745.

5. Mohammad F, Pandey GK, Mondal T, Enroth S, Redrup L, Gyllensten U, Kanduri C. *Long noncoding RNA-mediated maintenance of DNA methylation and transcriptionalgene silencing*. Development. 2012 Aug;139(15):2792-803. doi: 10.1242/dev.079566. PubMed PMID: 22721776

6. Kaikkonen MU, Lam MT, Glass CK. *Non-coding RNAs as regulators of gene expression and epigenetics.* Cardiovasc Res. 2011 Jun 1;90(3):430-40. doi:10.1093/cvr/cvr097. Review. PubMed PMID: 21558279; PubMed Central PMCID:PMC3096308.

7. Deaton AM, Bird A. *CpG islands and the regulation of transcription*. Genes Dev.2011 May 15;25(10):1010-22. doi: 10.1101/gad.2037511. Review. PubMed PMID:21576262; PubMed Central PMCID: PMC3093116.

8. Jenuwein T, Allis CD. *Translating the histone code*. Science. 2001 Aug10;293(5532):1074-80. Review. PubMed PMID: 11498575.

9. Zhang Y, Reinberg D. *Transcription regulation by histone methylation: interplay between different covalent modifications of the core histone tails.* Genes Dev. 2001 Sep 15;15(18):2343-60. Review. PubMed PMID: 11562345.

10. Lepikhov K, Walter J. *Differential dynamics of histone H3 methylation at positions K4 and K9 in the mouse zygote.* BMC Dev Biol. 2004 Sep 21;4:12. PubMed PMID: 15383155; PubMed Central PMCID: PMC521682.

11. Liu H, Kim JM, Aoki F. *Regulation of histone H3 lysine 9 methylation in oocytes and early pre-implantation embryos*. Development. 2004May;131(10):2269-80. PubMed PMID: 15102709.

12. Kourmouli N, Jeppesen P, Mahadevhaiah S, Burgoyne P, Wu R, Gilbert DM,Bongiorni S, Prantera G, Fanti L, Pimpinelli S, Shi W, Fundele R, Singh PB. *Heterochromatin and tri-methylated lysine 20 of histone H4 in animals*. J Cell Sci. 2004 May 15;117(Pt 12):2491-501. PubMed PMID: 15128874.

13. Adenot PG, Mercier Y, Renard JP, Thompson EM. *Differential H4 acetylation of paternal and maternal chromatin precedes DNA replication and differential transcriptional activity in pro-nuclei of 1-cell mouse embryos*. Development. 1997 Nov;124(22):4615-25. PubMed PMID: 9409678.

14. Hamilton AJ, Baulcombe DC. *A species of small antisense RNA in post-transcriptional gene silencing in plants*. Science. 1999 Oct29;286(5441):950-2. PubMed PMID: 10542148.

15. Dalmay T, Hamilton A, Mueller E, Baulcombe DC. *Potato virus X amplicons in arabidopsis mediate genetic and epigenetic gene silencing*. Plant Cell. 2000Mar;12(3):369-79. PubMed PMID: 10715323; PubMed Central PMCID: PMC139837.

16. Jones L, Hamilton AJ, Voinnet O, Thomas CL, Maule AJ, Baulcombe DC. *RNA-DNA interactions and DNA methylation in post-transcriptional gene silencing*. Plant Cell. 1999 Dec;11(12):2291-301. PubMed PMID: 10590159; PubMed Central PMCID:PMC144133.

17. Mette MF, van der Winden J, Matzke MA, Matzke AJ. *Production of aberrant promoter transcripts contributes to methylation and silencing of unlinked homologous promoters in trans*. EMBO J. 1999 Jan 4;18(1):241-8. PubMed PMID:9878066; PubMed Central PMCID: PMC1171118.

18. Volpe TA, Kidner C, Hall IM, Teng G, Grewal SI, Martienssen RA. *Regulation of heterochromatic silencing and histone H3 lysine-9 methylation by RNAi*. Science.2002 Sep 13;297(5588):1833-7. PubMed PMID: 12193640.

19. Reinhart BJ, Bartel DP. *Small RNAs correspond to centromere hetero chromatic repeats*. Science. 2002 Sep 13;297(5588):1831. PubMed PMID: 12193644.

20. Matzke M, Matzke AJ, Kooter JM. *RNA: guiding gene silencing*. Science. 2001 Aug10;293(5532):1080-3. PubMed PMID: 11498576.

21. Henikoff S, Matzke MA. *Exploring and explaining epigenetic effects*. Trends Genet. 1997 Aug;13(8):293-5. PubMed PMID: 9260513.

22. Hirabayashi Y, Gotoh Y. *Epigenetic control of neural precursor cell fate during development*. Nat Rev Neurosci. 2010 Jun;11(6):377-88. doi:10.1038/nrn2810. Review. PubMed PMID: 20485363.

23. Guy J, Cheval H, Selfridge J, Bird A. *The role of MeCP2 in the brain*. Annu. Rev Cell Dev Biol. 2011;27:631-52. doi: 10.1146/annurev-cellbio-092910-154121.Review. PubMed PMID: 21721946.

24. Jakovcevski M, Akbarian S. *Epigenetic mechanisms in neurological disease*. Nat Med. 2012 Aug;18(8):1194-204. doi: 10.1038/nm.2828. Review. PubMed PMID:22869198; PubMed Central PMCID: PMC3596876.

25. Yu NK, Baek SH, Kaang BK. *DNA methylation-mediated control of learning and memory*. Mol Brain. 2011 Jan 19;4:5. doi: 10.1186/1756-6606-4-5. Review. PubMedPMID: 21247469; PubMed Central PMCID: PMC3033800.

26. Day JJ, Sweatt JD. *DNA methylation and memory formation*. Nat Neurosci. 2010Nov;13(11):1319-23. doi: 10.1038/nn.2666. PubMed PMID: 20975755; PubMed CentralPMCID: PMC3130618.

27. Borrelli E, Nestler EJ, Allis CD, Sassone-Corsi P. *Decoding the epigenetic language of neuronal plasticity*. Neuron. 2008 Dec 26;60(6):961-74. doi:10.1016/j.neuron.2008.10.012. Review. PubMed PMID: 19109904; PubMed CentralPMCID: PMC2737473.

28. Tsankova N, Renthal W, Kumar A, Nestler EJ. *Epigenetic regulation in psychiatric disorders*. Nat Rev Neurosci. 2007 May;8(5):355-67. Review. PubMedPMID: 17453016.

29. Mill J, Tang T, Kaminsky Z, Khare T, Yazdanpanah S, Bouchard L, Jia P,Assadzadeh A, Flanagan J, Schumacher A, Wang SC, Petronis A. *Epigenomic profiling reveals DNA-methylation changes associated with major psychosis*. Am J Hum Genet. 2008 Mar;82(3):696-711. doi: 10.1016/j.ajhg.2008.01.008. PubMed PMID: 18319075;PubMed Central PMCID: PMC2427301.

30. Keller S, Sarchiapone M, Zarrilli F, Videtic A, Ferraro A, Carli V, Sacchetti S, Lembo F, Angiolillo A, Jovanovic N, Pisanti F, Tomaiuolo

R, Monticelli A,Balazic J, Roy A, Marusic A, Cocozza S, Fusco A, Bruni CB, Castaldo G, ChiariottiL. *Increased BDNF promoter methylation in the Wernicke area of suicide subjects.* Arch Gen Psychiatry. 2010 Mar;67(3):258-67. doi:10.1001/archgenpsychiatry.2010.9. PubMed PMID: 20194826.

31. Labonté B, Suderman M, Maussion G, Navaro L, Yerko V, Mahar I, Bureau A,Mechawar N, Szyf M, Meaney MJ, Turecki G. *Genome-wide epigenetic regulation by early-life trauma*. Arch Gen Psychiatry. 2012 Jul;69(7):722-31. doi:10.1001/archgenpsychiatry.2011.2287. PubMed PMID: 22752237; PubMed Central PMCID:PMC4991944.

32. Lutz PE, Almeida D, Fiori LM, Turecki G. *Childhood maltreatment and stress-related psychopathology: the epigenetic memory hypothesis*. Curr Pharm Des.2015;21(11):1413-7. Review. PubMed PMID: 25564388.

33. Bird A. *DNA methylation patterns and epigenetic memory*. Genes Dev. 2002 Jan1;16(1):6-21. Review. PubMed PMID: 11782440.

34. Wilson GG, Murray NE. *Restriction and modification systems*. Annu Rev Genet.1991;25:585-627. Review. PubMed PMID: 1812816.

35. Wolf SF, Jolly DJ, Lunnen KD, Friedmann T, Migeon BR. *Methylation of the hypoxanthine phosphoribosyl transferase locus on the human X chromosome: implications for X-chromosome inactivation.* Proc Natl Acad Sci U S A. 1984May;81(9):2806-10. PubMed PMID: 6585829; PubMed Central PMCID: PMC345159.

36. Cotton AM, Lam L, Affleck JG, Wilson IM, Peñaherrera MS, McFadden DE, KoborMS, Lam WL, Robinson WP, Brown CJ. *Chromosome-wide DNA methylation analysis predicts human tissue-specific X inactivation*. Hum Genet. 2011Aug;130(2):187-201. doi: 10.1007/s00439-011-1007-8. PubMed PMID: 21597963; PubMedCentral PMCID: PMC3132437.

37. Weaver JR, Susiarjo M, Bartolomei MS. *Imprinting and epigenetic changes in the early embryo*. Mamm Genome. 2009 Sep-Oct;20(9-10):532-43. doi:10.1007/s00335-009-9225-2. Review. PubMed PMID: 19760320.

38. Russo G, Landi R, Pezone A, Morano A, Zuchegna C, Romano A, Muller MT,Gottesman ME, Porcellini A, Avvedimento EV. DNA damage and Repair Modify DNA methylation and Chromatin Domain of the Targeted Locus: Mechanism of allele methylation polymorphism. Sci Rep. 2016 Sep 15;6:33222. doi: 10.1038/srep33222.PubMed PMID: 27629060; PubMed Central PMCID: PMC5024116.

39. Cholewa-Waclaw J, Bird A, von Schimmelmann M, Schaefer A, Yu H, Song H, Madabhushi R, Tsai LH. *The Role of Epigenetic Mechanisms in the Regulation of Gene Expression in the Nervous System*. J Neurosci. 2016 Nov 9;36(45):11427-11434.PubMed PMID: 27911745; PubMed Central PMCID: PMC5125210.

40. Okano M, Xie S, Li E. *Cloning and characterization of a family of novel mammalian DNA (cytosine-5) methyltransferases*. Nat Genet. 1998 Jul;19(3):219-20. PubMed PMID: 9662389.

41. Yen RW, Vertino PM, Nelkin BD, Yu JJ, el-Deiry W, Cumaraswamy A, Lennon GG,Trask BJ, Celano P, Baylin SB. *Isolation and characterization of the cDNA encoding human DNA methyltransferase*. Nucleic Acids Res. 1992 May11;20(9):2287-91. PubMed PMID: 1594447; PubMed Central PMCID: PMC312343.

42. Antequera F, Macleod D, Bird AP. *Specific protection of methylated CpGs in mammalian nuclei*. Cell. 1989 Aug 11;58(3):509-17. PubMed PMID: 2474378.

43. Lewis JD, Meehan RR, Henzel WJ, Maurer-Fogy I, Jeppesen P, Klein F, Bird A. *Purification, sequence, and cellular localization of a novel chromosomal protein that binds to methylated DNA*. Cell. 1992 Jun 12;69(6):905-14. PubMed PMID:1606614.

44. Moretti P, Zoghbi HY. *MeCP2 dysfunction in Rett syndrome and related disorders*. Curr Opin Genet Dev. 2006 Jun;16(3):276-81. Review. PubMed PMID:16647848.

45. Guo W, Zhang MQ, Wu H. *Mammalian non-CG methylations are conserved and cell-type specific and may have been involved in the evolution of transposon elements*. Sci Rep. 2016 Aug 30;6:32207. doi: 10.1038/srep32207. PubMed PMID:27573482; PubMed Central PMCID: PMC5004121.

46. Lister R, Pelizzola M, Kida YS, Hawkins RD, Nery JR, Hon G,Antosiewicz-Bourget J, O'Malley R, Castanon R, Klugman S, Downes M, Yu R, StewartR, Ren B, Thomson JA, Evans RM, Ecker JR. *Hotspots of aberrant epigenomic reprogramming in human induced pluripotent stem cells*. Nature. 2011 Mar3;471(7336):68-73. doi: 10.1038/nature09798. Erratum in: Nature. 2014 Oct2;514(7520):126. PubMed PMID: 21289626; PubMed Central PMCID: PMC3100360.

47. Ziller MJ, Müller F, Liao J, Zhang Y, Gu H, Bock C, Boyle P, Epstein CB,Bernstein BE, Lengauer T, Gnirke A, Meissner A. *Genomic*

distribution and inter-sample variation of non-CpG methylation across human cell types. PLoSGenet. 2011 Dec;7(12):e1002389. doi: 10.1371/journal.pgen.1002389. PubMed PMID:22174693; PubMed Central PMCID: PMC3234221.

48. Lister R, Mukamel EA, Nery JR, Urich M, Puddifoot CA, Johnson ND, Lucero J,Huang Y, Dwork AJ, Schultz MD, Yu M, Tonti-Filippini J, Heyn H, Hu S, Wu JC, Rao A, Esteller M, He C, Haghighi FG, Sejnowski TJ, Behrens MM, Ecker JR. *Global epigenomic reconfiguration during mammalian brain development*. Science. 2013 Aug 9;341(6146):1237905. doi: 10.1126/science.1237905. PubMed PMID: 23828890; PubMed Central PMCID: PMC3785061.

49. Xie W, Barr CL, Kim A, Yue F, Lee AY, Eubanks J, Dempster EL, Ren B.*Base-resolution analyses of sequence and parent-of-origin dependent DNA methylation in the mouse genome*. Cell. 2012 Feb 17;148(4):816-31. doi:10.1016/j.cell.2011.12.035. PubMed PMID: 22341451; PubMed Central PMCID:PMC3343639.

50. Pastor WA, Aravind L, Rao A. *TETonic shift: biological roles of TET protein sin DNA demethylation and transcription*. Nat Rev Mol Cell Biol. 2013Jun;14(6):341-56. doi: 10.1038/nrm3589. Review. PubMed PMID: 23698584; PubMedCentral PMCID: PMC3804139

51. Ito S, Shen L, Dai Q, Wu SC, Collins LB, Swenberg JA, He C, Zhang Y. *Tet proteins can convert 5-methylcytosine to 5-formylcytosine and 5-carboxylcytosine*.Science. 2011 Sep 2;333(6047):1300-3. doi: 10.1126/science.1210597. PubMed PMID: 21778364; PubMed Central PMCID: PMC3495246.

52. Guo JU, Su Y, Zhong C, Ming GL, Song H. *Hydroxylation of 5-methylcytosine by TET1 promotes active DNA demethylation in the adult brain*. Cell. 2011 Apr29;145(3):423-34. doi: 10.1016/j.cell.2011.03.022. PubMed PMID: 21496894; PubMed Central PMCID: PMC3088758.

53. Mo A, Mukamel EA, Davis FP, Luo C, Henry GL, Picard S, Urich MA, Nery JR,Sejnowski TJ, Lister R, Eddy SR, Ecker JR, Nathans J. *Epigenomic Signatures of Neuronal Diversity in the Mammalian Brain. Neuron*. 2015 Jun 17;86(6):1369-84.doi: 10.1016/j.neuron.2015.05.018. PubMed PMID: 26087164; PubMed Central PMCID:PMC4499463.

54. Clark SJ, Statham A, Stirzaker C, Molloy PL, Frommer M. *DNA methylation: bisulphite modification and analysis*. Nat Protoc. 2006;1(5):2353-64. PubMed PMID:17406479.

55. Lee EJ, Pei L, Srivastava G, Joshi T, Kushwaha G, Choi JH, Robertson KD, Wang X, Colbourne JK, Zhang L, Schroth GP, Xu D, Zhang K, Shi H. *Targeted bisulfite sequencing by solution hybrid selection and massively parallel sequencing*. Nucleic Acids Res. 2011 Oct;39(19):e127. doi: 10.1093/nar/gkr598. PubMed PMID:21785137; PubMed Central PMCID: PMC3201883.

56. Arai Y, Fukukawa H, Atozi T, Matsumoto S, Hanazono Y, Nagashima H, Ohgane J. *Ultra-Deep Bisulfite Sequencing to Detect Specific DNA Methylation Patterns of Minor Cell Types in Heterogeneous Cell Populations: An Example of the Pituitary Tissue*. PLoS One. 2016 Jan 11;11(1):e0146498. doi: 10.1371/journal.pone.0146498. PubMed PMID: 26752725; PubMed Central PMCID: PMC4709138.

57. Lee EJ, Luo J, Wilson JM, Shi H. *Analyzing the cancer methylome through targeted bisulfite sequencing*. Cancer Lett. 2013 Nov 1;340(2):171-8. doi:10.1016/j.canlet.2012.10.040. Review. PubMed PMID: 23200671; PubMed CentralPMCID: PMC3616138.

58. Suzuki M, Jing Q, Lia D, Pascual M, McLellan A, Greally JM. *Optimized designand data analysis of tag-based cytosine methylation assays.* Genome Biol.2010;11(4):R36. doi: 10.1186/gb-2010-11-4-r36. PubMed PMID: 20359321; PubMedCentral PMCID: PMC2884539.

59. Claus R, Wilop S, Hielscher T, Sonnet M, Dahl E, Galm O, Jost E, Plass C. *A systematic comparison of quantitative high-resolution DNA methylation analysis and methylation-specific PCR*. Epigenetics. 2012 Jul;7(7):772-80. doi:10.4161/epi.20299. PubMed PMID: 22647397; PubMed Central PMCID: PMC3414395.

60. Maussion G, Yang J, Suderman M, Diallo A, Nagy C, Arnovitz M, Mechawar N,Turecki G. *Functional DNA methylation in a transcript specific 3'UTR region of TrkB associates with suicide*. Epigenetics. 2014 Aug;9(8):1061-70. doi:10.4161/epi.29068. PubMed PMID: 24802768; PubMed Central PMCID: PMC4164491.

61. Draht MX, Smits KM, Jooste V, Tournier B, Vervoort M, Ramaekers C, Chapusot C,Weijenberg MP, van Engeland M, Melotte V. *Analysis of RET promoter CpG island methylation using methylation-specific PCR (MSP), pyrosequencing, and methylation-sensitive high-resolution melting (MS-HRM): impact on stage II colon cancer patient outcome*. Clin Epigenetics. 2016 Apr 26;8:44. doi:10.1186/s13148-016-0211-8. PubMed PMID: 27118999; PubMed Central PMCID:PMC4845472.

62. Teh AL, Pan H, Lin X, Lim YI, Patro CP, Cheong CY, Gong M, MacIsaac JL, KwohCK, Meaney MJ, Kobor MS, Chong YS, Gluckman

PD, Holbrook JD, Karnani N. *Comparison of Methyl-capture Sequencing vs. Infinium 450K methylation array formethylome analysis in clinical samples*. Epigenetics.2016;11(1):3648.doi:10.1080/15592294.2015.1132136.Pub Med PMID: 26786415; PubMed Central PMCID:PMC4846133.

63. Lee JH, Park SJ, Kenta N. *An integrative approach for efficient analysis ofwhole genome bisulfite sequencing data*. BMC Genomics. 2015;16 Suppl 12:S14. doi: 10.1186/1471-2164-16-S12-S14. PubMed PMID: 26680746; PubMed Central PMCID:PMC4682396.

64. Bretz CL, Langohr IM, Lee S, Kim J. *Epigenetic instability at imprinting control regions in a Kras(G12D)-induced T-cell neoplasm*. Epigenetics.2015;10(12):1111-20.doi:10.1080/15592294.2015.1110672. PubMed PMID: 26507119;PubMed Central PMCID: PMC4844204.

65. Kwon MJ, Kim S, Han MH, Lee SB. *Epigenetic Changes in Neurodegenerative Diseases*. Mol Cells. 2016 Nov 30;39(11):783-789. Review. PubMed PMID: 27871175;PubMed Central PMCID: PMC5125933.

66. Okae H, Chiba H, Hiura H, Hamada H, Sato A, Utsunomiya T, Kikuchi H, YoshidaH, Tanaka A, Suyama M, Arima T. *Genome-wide analysis of DNA methylation dynamics during early human development*. PLoS Genet.2014 Dec11;10(12):e1004868. doi:10.1371/journal.pgen.1004868. PubMed PMID: 25501653; PubMed Central PMCID:PMC4263407.

67. Numata,S., Ye,T., Hyde,T.M., Guitart-Navarro,X., Tao,R., Wininger,M., Colantuoni,C., Weinberger,D.R., Kleinman,J.E. and Lipska,B.K. *DNA methylation signatures in development and aging of the human prefrontal cortex*. Am. J. Hum. Genet., 2012 90, 260-272.

68. Akbarian,S. and Nestler,E.J. *Epigenetic mechanisms in psychiatry*. Neuropsychopharmacology, 2013 38, 1-2.

69. Miller,G. *Epigenetics. The seductive allure of behavioral epigenetics.* Science, 2010 329, 24-27.

70. Perroud,N., Salzmann,A., Prada,P., Nicastro,R., Hoeppli,M.E., Furrer,S., Ardu,S., Krejci,I., Karege,F. and Malafosse,A. *Response to psychotherapy in borderline personality disorder and methylation status of the BDNF gene*. Transl. Psychiatry, 2013 3, e207.

71. Nestler,E.J., Peña,C.J., Kundakovic,M., Mitchell,A. and Akbarian,S. *Epigenetic Basis of Mental Illness*. Neuroscientist, (2015) pii: 1073858415608147.

72. Labonté,B., Suderman,M., Maussion,G., Navaro,L., Yerko,V., Mahar,I., Bureau,A., Mechawar,N., Szyf,M., Meaney,M.J. and Turecki,G. *Genome-wide epigenetic regulation by early-life trauma.* Arch. Gen. Psychiatry, 2012 69, 722-731.

73. Qu W, Tsukahara T, Nakamura R, Yurino H, Hashimoto S, Tsuji S, Takeda H,Morishita S. *Assessing Cell-to-Cell DNA Methylation Variability on Individual Long Reads*. Sci Rep. 2016 Feb 18;6:21317. doi: 10.1038/srep21317. PubMed PMID:26888466; PubMed Central PMCID: PMC4758075.

74. Li S, Garrett-Bakelman F, Perl AE, Luger SM, Zhang C, To BL, Lewis ID, BrownAL, D'Andrea RJ, Ross ME, Levine R, Carroll M, Melnick A, Mason CE. *Dynamic evolution of clonal epialleles revealed by methclone.* Genome Biol. 2014 Sep27;15(9):472. doi: 10.1186/s13059-014-0472-5. PubMed PMID: 25260792; PubMedCentral PMCID: PMC4242486.

75. Landan G, Cohen NM, Mukamel Z, Bar A, Molchadsky A, Brosh R, Horn-Saban S,Zalcenstein DA, Goldfinger N, Zundelevich A, Gal-Yam EN, Rotter V, Tanay A. *Epigenetic polymorphism and the stochastic formation of differentially methylated regions in normal and cancerous tissues*. Nat Genet. 2012 Nov;44(11):1207-14. doi:10.1038/ng.2442. PubMed PMID: 23064413.

76. Punzo D, Errico F, Cristino L, Sacchi S, Keller S, Belardo C, Luongo L, Nuzzo T, Imperatore R, Florio E, De Novellis V, Affinito O, Migliarini S, Maddaloni G, Sisalli MJ, Pasqualetti M, Pollegioni L, Maione S, Chiariotti L, Usiello A. *Age-Related Changes in D-Aspartate Oxidase Promoter Methylation Control Extracellular D-Aspartate Levels and Prevent Precocious Cell Death during BrainAging*. J Neurosci. 2016 Mar 9;36(10):3064-78. doi:10.1523/JNEUROSCI.3881-15.2016. PubMed PMID: 26961959.

77. Sisalli MJ, Secondo A, Esposito A, Valsecchi V, Savoia C, Di Renzo GF, Annunziato L, Scorziello A. *Endoplasmic reticulum refilling and mitochondrial calcium extrusion promoted in neurons by NCX1 and NCX3 in ischemic preconditioning are determinant for neuroprotection*. Cell Death Differ 2014; 21: 1142-9.

78. Boscia F, D'Avanzo C, Pannaccione A, Secondo A, Casamassa A, Formisano L, Guida N, Sokolow S, Herchuelz A, Annunziato L.

Silencing or knocking out the Na(+)/Ca(2+) exchanger-3 (NCX3) impairs oligodendrocyte differentiation. Cell Death Differ 2012; 19: 562-72.

79. Boscia F, Esposito CL, Casamassa A, de Franciscis V, Annunziato L, Cerchia L. *The isolectin IB4 binds RET receptor tyrosine kinase in microglia*. J Neurochem 2013; 126: 428-36.

80. Fico A, Manganelli G, Simeone M, Guido S, Minchiotti G, Filosa S. *High-throughput screening-compatible single-step protocol to differentiate embryonic stem cells in neurons*. Stem Cells Dev 2008; 17: 573-84

81. Colucci-D'Amato GL, Tino A, Pernas-Alonso R, ffrench-Mullen JM, di Porzio U. *Neuronal and glial properties coexist in a novel mouse CNS immortalized cell line*. Exp Cell Res 1999; 252: 383-91

82. Zhang J, Kobert K, Flouri T, Stamatakis A. *PEAR: a fast and accurate Illumina Paired-End reAd mergeR*. Bioinformatics 2013; 30: 614-20

83. Schmieder R, Edwards R. *Quality control and preprocessing of metagenomic datasets*. Bioinformatics 2011; 27: 863-4.

84. Scala G, Affinito O, Palumbo D, Florio E, Monticelli A, Miele G, Chiariotti L,Cocozza S. *ampliMethProfiler: a pipeline for the analysis of CpG methylationprofiles of targeted deep bisulfite sequenced amplicons*. BMC Bioinformatics. 2016Nov 25;17(1):484. PubMed PMID: 27884103; PubMed Central PMCID: PMC5123276.

85. Camacho C, Coulouris G, Avagyan V, Ma N, Papadopoulos J, Bealer K, Madden TL. *BLAST+: architecture and applications*. BMC Bioinformatics 2009; 10: 421.

86. Errico F, D'Argenio V, Sforazzini F, Iasevoli F, Squillace M, Guerri G, Napolitano F, Angrisano T, Di Maio A, Keller S, et al. *A role for D-aspartate oxidase in schizophrenia and in schizophrenia-related symptoms induced by phencyclidine in mice*. Transl Psychiatry 2015; 5:e512.

87. McGowan,P.O. and Szyf,M. *The epigenetics of social adversity in early life: implications for mental health outcomes*. Neurobiol. Dis., 2010 39, 66-72.

88. Mikeska,T., Candiloro,I.L. and Dobrovic,A. *The implications of heterogeneous DNA methylation for the accurate quantification of methylation*. Epigenomics, 2010 2, 561-573.

89. Candiloro,I.L., Mikeska,T. and Dobrovic,A. *Assessing combined methylation-sensitive high resolution melting and pyrosequencing for the analysis of heterogeneous DNA methylation*. Epigenetics, 2011 6, 500-507.

90. Wee,E.J., Rauf,S., Shiddiky,M.J., Dobrovic,A. and Trau,M. *DNA ligase-based strategy for quantifying heterogeneous DNA methylation without sequencing*. Clin. Chem., 2015 61, 163-171.

91. Li,S., Garrett-Bakelman,F.E., Chung,S.S., Sanders,M.A., Hricik,T., Rapaport,F., Patel,J., Dillon,R., Vijay,P., Brown,A.L. et al. *Distinct evolution and dynamics of epigenetic and genetic heterogeneity in acute myeloid leukemia.* Nat. Med., 2016 10.1038/nm.4125.

92. Schübeler,D. *Function and information content of DNA methylation*. Nature, 2015 517, 321-326.

93. Aguilar CA, Craighead HG. *Micro and nanoscale devices for the investigation of epigenetics and chromatin dynamics*. Nat Nanotechnol., 2013 Oct; 8(10): 709-718.

94. Florio E, Keller S, Coretti L, Affinito O, Scala G, Errico F, Fico A, Boscia F, Sisalli MJ, Reccia MG, Miele G, Monticelli A, Scorziello A, Lembo F, Colucci-D'Amato L, Minchiotti G, Avvedimento VE, Usiello A, Cocozza S, Chiariotti L. *Tracking the evolution of epialleles during neural differentiation and brain development: D-Aspartate oxidase as a model gene*. Epigenetics. 2017 Jan 2; 12(1):41-54.

Affermo con la presente che questa sottomissione è frutto del mio lavoro e che, al meglio della mia conoscenza e convinzione, non contiene materiale precedentemente pubblicato o scritto da un'altra persona, tranne dove il riconoscimento dovuto è stato fatto nel testo. Parte del lavoro di tesi qui riportato è stato oggetto di pubblicazione da parte del sottoscritto et al (Florio et al. 2017 Ref. 94); alcune figure derivano dalla suddetta pubblicazione scientifica.

List of publication

I. Chiariotti L, Angrisano T, Keller S, **Florio E**, Affinito O, Pallante P, Perrino C, Pero R, Lembo F. Epigenetic modifications induced by Helicobacter pylori infection through a direct microbe-gastric epithelial cells cross-talk. Med Microbiol Immunol. May 29 -2013

II. Keller S, Angrisano T, **Florio E**, Pero R, Decaussin□Petrucci M, Troncone G, Capasso M, Lembo F, Fusco A, Chiariotti L*; DNA methylation state of the galectin-3 gene represents a potential new marker of thyroid malignancy*. **Oncology letters** .(86-90) Volume 6 Number 1.z July 2013

III. Zarrilli F, Zarrilli F, Amato F, Castaldo G, Tomaiuolo R, Keller S, **Florio E**, ChiariottiL, Carli V, Stuppia L, Sarchiapone M. *Tropomyosin-related kinase B receptor polymorphisms and isoforms expression in suicide victims*. **Psychiatry Res**. 2014 Dec 15;220(1-2):725-6.

IV. Angrisano T, Schiattarella GG, Keller S, Pironti G, **Florio E**, Magliulo F,Bottino R, Pero R, Lembo F, Avvedimento EV, Esposito G, Trimarco B, Chiariotti L,Perrino C. *Epigenetic switch at atp2a2 and myh7 gene promoters in pressure overload-induced heart failure*. **PLoS One**. 2014 Sep 2;9(9):e106024.

V. Keller S, Errico F, Zarrilli F, **Florio E**, Punzo D, Mansueto S, Angrisano T,Pero R, Lembo F, Castaldo G, Usiello A, Chiariotti L. *DNA methylation state of BDNF gene is not altered in prefrontal cortex and striatum of schizophrenia subjects*. **Psychiatry Res.** 2014 Dec 30;220(3):1147-50.

VI. Punzo D, Errico F, Cristino L, Sacchi S, Keller S, Belardo C, Luongo L, Nuzzo T, Imperatore R, **Florio E**, De Novellis V, Affinito O, Migliarini S, Maddaloni G, Sisalli MJ, Pasqualetti M, Pollegioni L, Maione S, Chiariotti L, Usiello A. Age-Related Changes in d-Aspartate Oxidase Promoter Methylation Control Extracellular d-Aspartate Levels and Prevent Precocious Cell Death during Brain Aging. **Journal of Neuroscience** 2016 Mar 9;36(10):3064-78

VII. Angrisano T, Pero R, Brancaccio M, Coretti L, **Florio E**, Pezone A, Calabrò V, Falco G, Keller S, Lembo F, Avvedimento VE, Chiariotti L. Cyclical DNA Methylation and Histone Changes Are Induced by LPS to Activate COX-2 in Human Intestinal Epithelial Cells. **PLoS One**. 2016 Jun 2;11(6):e0156671

VIII. Affinito O, Scala G, Palumbo D**, Florio E**, Monticelli A, Miele G, Avvedimento VE, Usiello A, Chiariotti L, Cocozza S. Modeling DNA methylation by analyzing the individual configurations of single molecules. **Epigenetics**. 2016 Oct 17:1-8.

IX. **Florio E**, Keller S, Coretti L, Affinito O, Scala G, Errico F, Fico A, Boscia F, Sisalli MJ, Reccia MG, Miele G, Monticelli A, Scorziello A, Lembo F, Colucci-

D'Amato L, Minchiotti G, Avvedimento VE, Usiello A, Cocozza S, Chiariotti L. Tracking the evolution of epialleles during neural differentiation and brain development: D-Aspartate oxidase as a model gene. **Epigenetics**. 2017 Jan 2;12(1):41-54.

X. Scala G, Affinito O, Palumbo D, **Florio E**, Monticelli A, Miele G, Chiariotti L, Cocozza S. ampliMethProfiler: a pipeline for the analysis of CpG methylation profiles of targeted deep bisulfite sequenced amplicons. BMC Bioinformatics. 2016 Nov 25;17(1):484.

XI. Coretti L, Cuomo M, **Florio E**, Palumbo D, Keller S, Pero R, Chiariotti L, Lembo F and Cafiero C. Subgingival dysbiosis in smoker and non-smoker patients with chronic periodontitis. Molecular Medicine Reports March 2017

XII. Coretti L., Natale A., Cuomo M., **Florio E**., Keller S., Lembo F., Chiariotti L. and Pero R. The Interplay Between Defensins and Microbiota in Crohn's Disease. Mediators of inflammation Jan 2017

XIII. Coretti l., Cristiano C, **Florio E**., Scala G., Lama A., Keller S., Cuomo M., Russo R., Pero R., Mattace Raso G., Meli R., Cocozza S., Calignano A., Chiariotti L. and Lembo F.. Sex-related alterations of gut microbiota composition in the BTBR mouse model of autism spectrum disorder. Scientific Reports F March 2017

XIV. Nuzzo T, Sacchi S, Errico F, Keller S, Palumbo O, Florio E, Punzo D, Napolitano F, Copetti M, Carella M, Chiariotti L, Pollegioni L and Usiello A. Decreased free D-aspartate levels are linked to enhanced D-aspartate oxidase activity in the dorsolateral prefrontal cortex of schizophrenia patients. NPJ. Schizophrenia Jan 2017.